

Tuning the Emission of Cationic Iridium (III) Complexes Towards the Red Through Methoxy Substitution of the Cyclometalating Ligand

Kamrul Hasan,^a Ashu K. Bansal,^b Ifor D.W. Samuel,^b Cristina Roldán-Carmona,^{c,d} Henk Bolink^{c*} and Eli Zysman-Colman^{e*}

^a Département de Chimie, Université de Sherbrooke, 2500 Boul. de l'Université, Sherbrooke, QC, Canada, J1K 2R1

^b Organic Semiconductor Centre, SUPA School of Physics and Astronomy, University of St. Andrews, North Haugh, St. Andrews, Fife, UK, KY16 9SS

^c Instituto de Ciencia Molecular, Universidad de Valencia, C/ Catedrático J. Beltrán 2, 46980 Paterna (Valencia), Spain. henk.bolink@uv.es

^d Department of Physical Chemistry and Applied Thermodynamics, Campus Rabanales, Ed. C3, University of Cordoba, 14014, Spain

^e Organic Semiconductor Centre, EaStCHEM School of Chemistry, University of St Andrews, St Andrews, Fife, UK, KY16 9ST, Fax: +44-1334 463808; Tel: +44-1334 463826; E-mail: eli.zysman-colman@st-andrews.ac.uk; URL: <http://www.zysman-colman.com>

SUPPORTING INFORMATION

Table of contents:

	Pages
¹ H and ¹³ C NMR spectrum of individual compounds and complexes	S2-S23
Synthesis of ligands	S24
Tables of electrochemical and UV-Visible absorption data	S24-S25
UV-vis and emission spectra of individual complexes	S26-S29
Cyclic voltammograms of individual complexes	S30-S33
TDDFT UV-Vis absorption spectra predictions	S34-S37
Performance of LEECs fabricated with 1a – 4b complexes	S38
References	S38

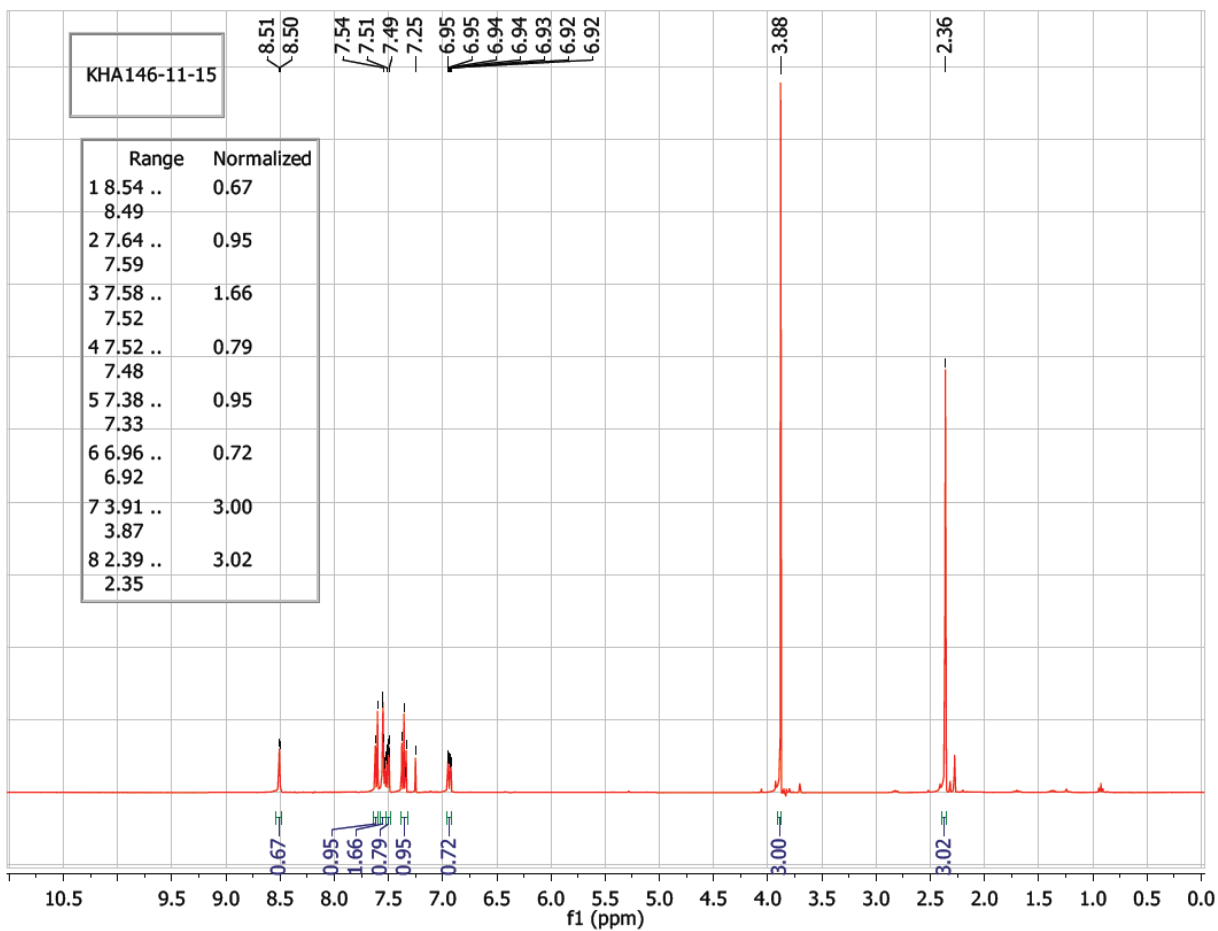


Figure S1. ^1H NMR spectrum of 2-(3'-Methoxyphenyl)-5-methylpyridine (**3-MeOppy**) in CDCl_3

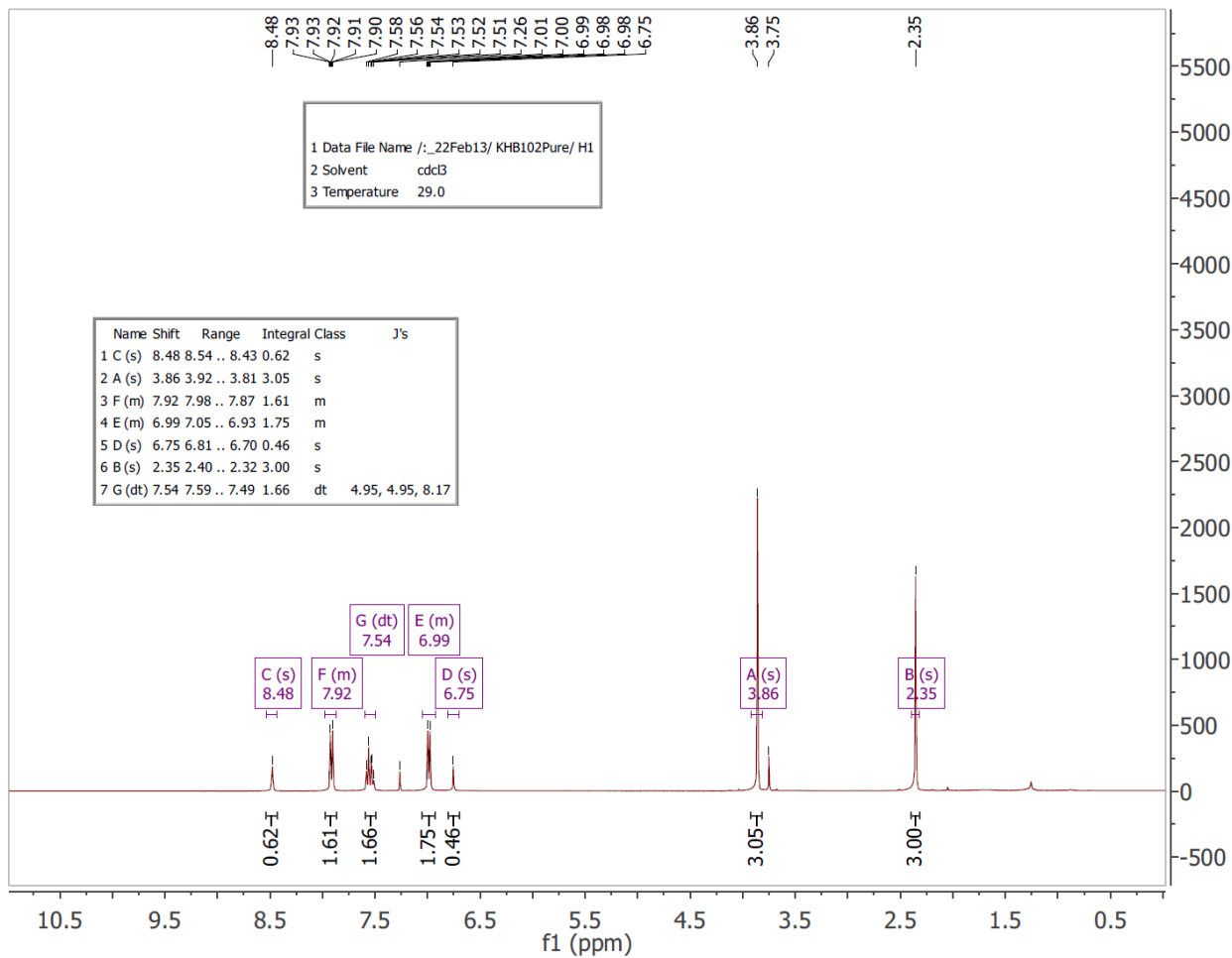


Figure S2. ^1H NMR spectrum of 2-(4'-Methoxyphenyl)-5-methylpyridine (4-MeOppy) in CDCl_3

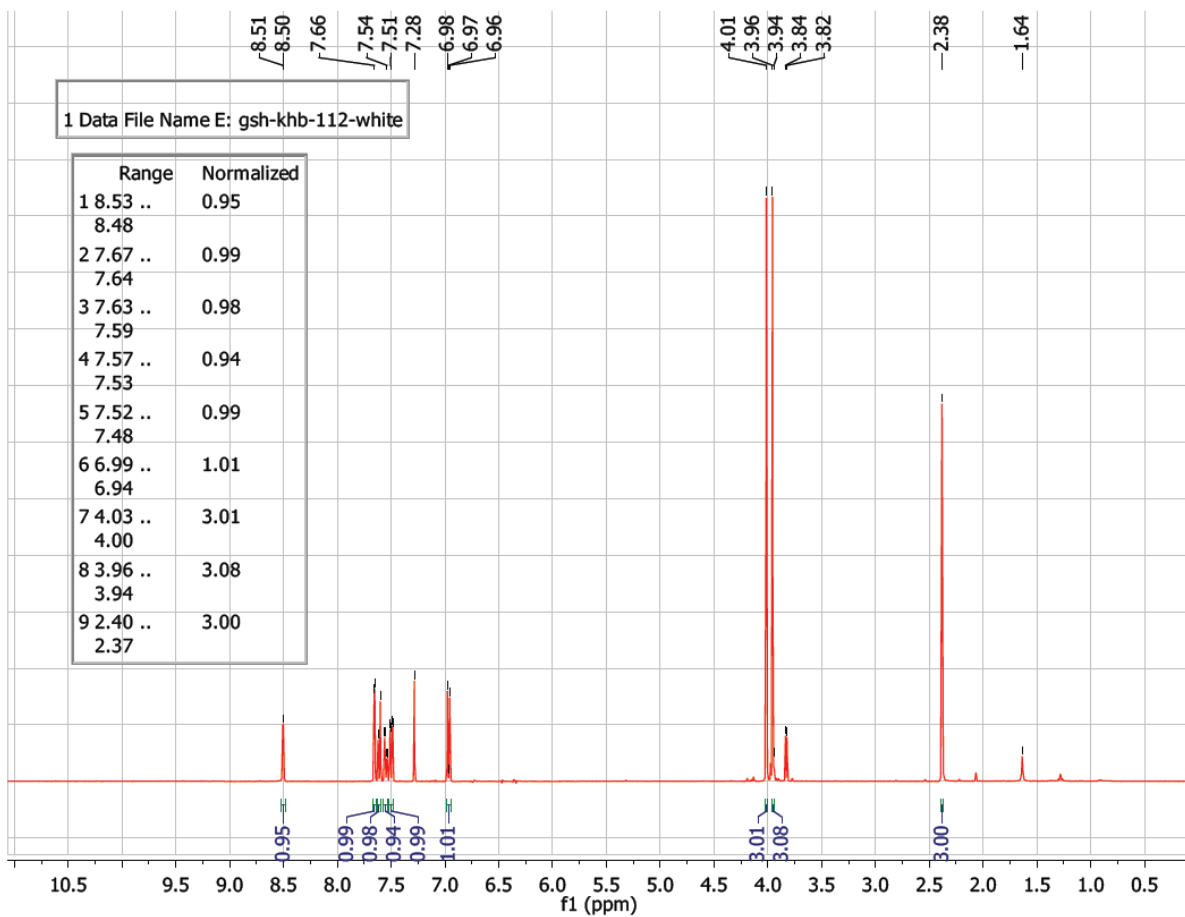


Figure S3. ^1H NMR spectrum of 2-(3',4'-Dimethoxyphenyl)-5-methylpyridine (3,4-dMeOppy) in CDCl_3

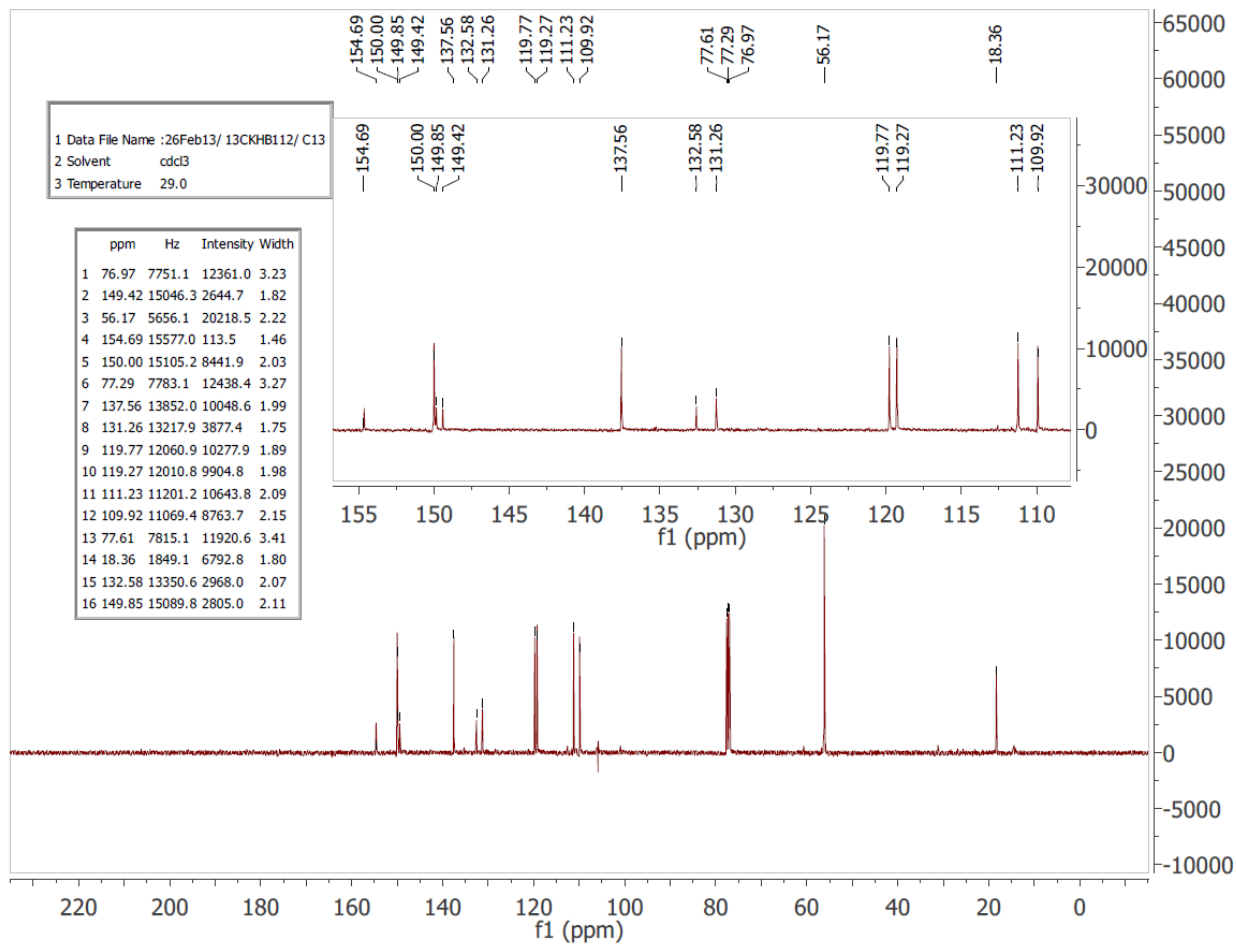


Figure S4. ^{13}C NMR spectrum of 2-(3',4'-Dimethoxyphenyl)-5-methylpyridine (**3,4-dMeOppy**) in CDCl_3

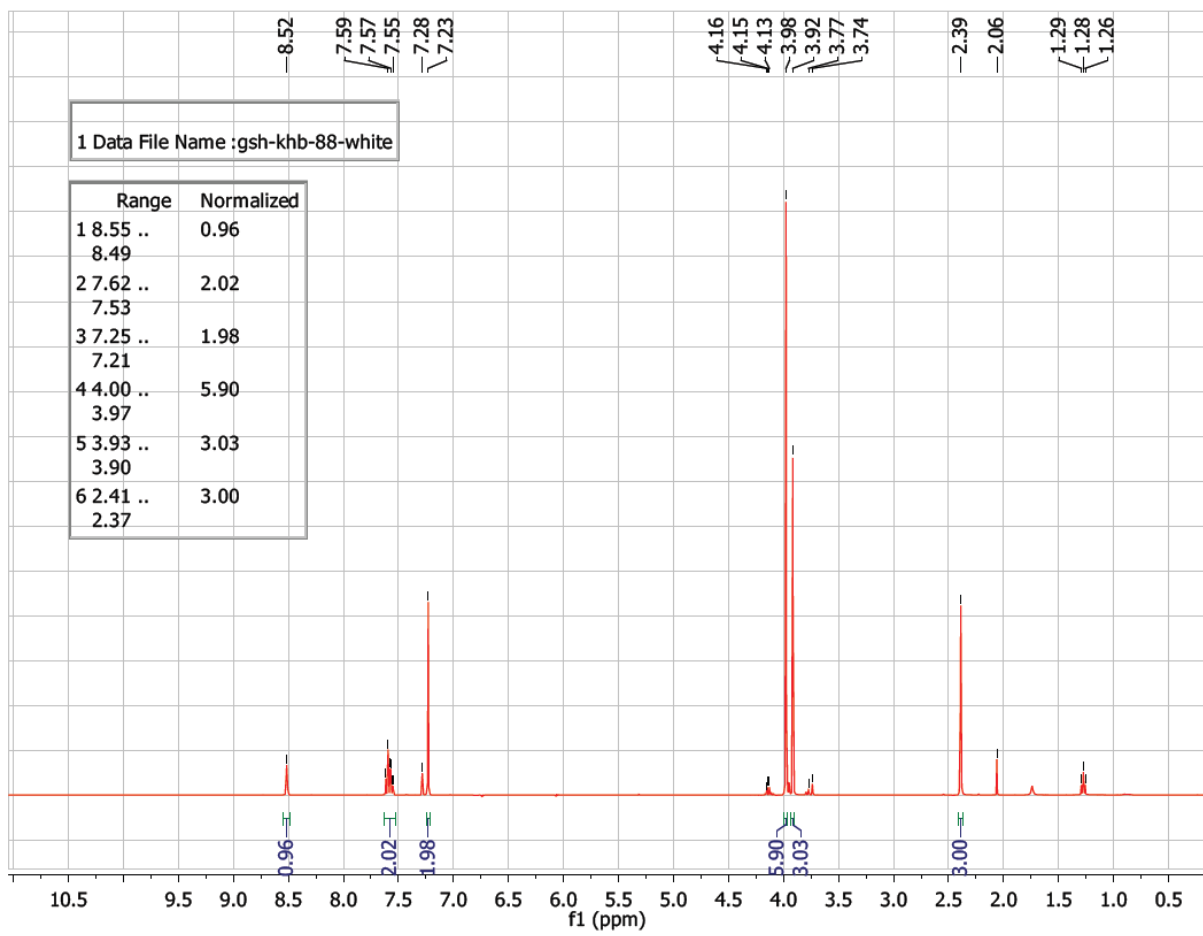


Figure S5. ^1H NMR spectrum of 2-(3',4',5'-Trimethoxyphenyl)-5-methylpyridine (3,4,5-tMeOppy) in CDCl_3

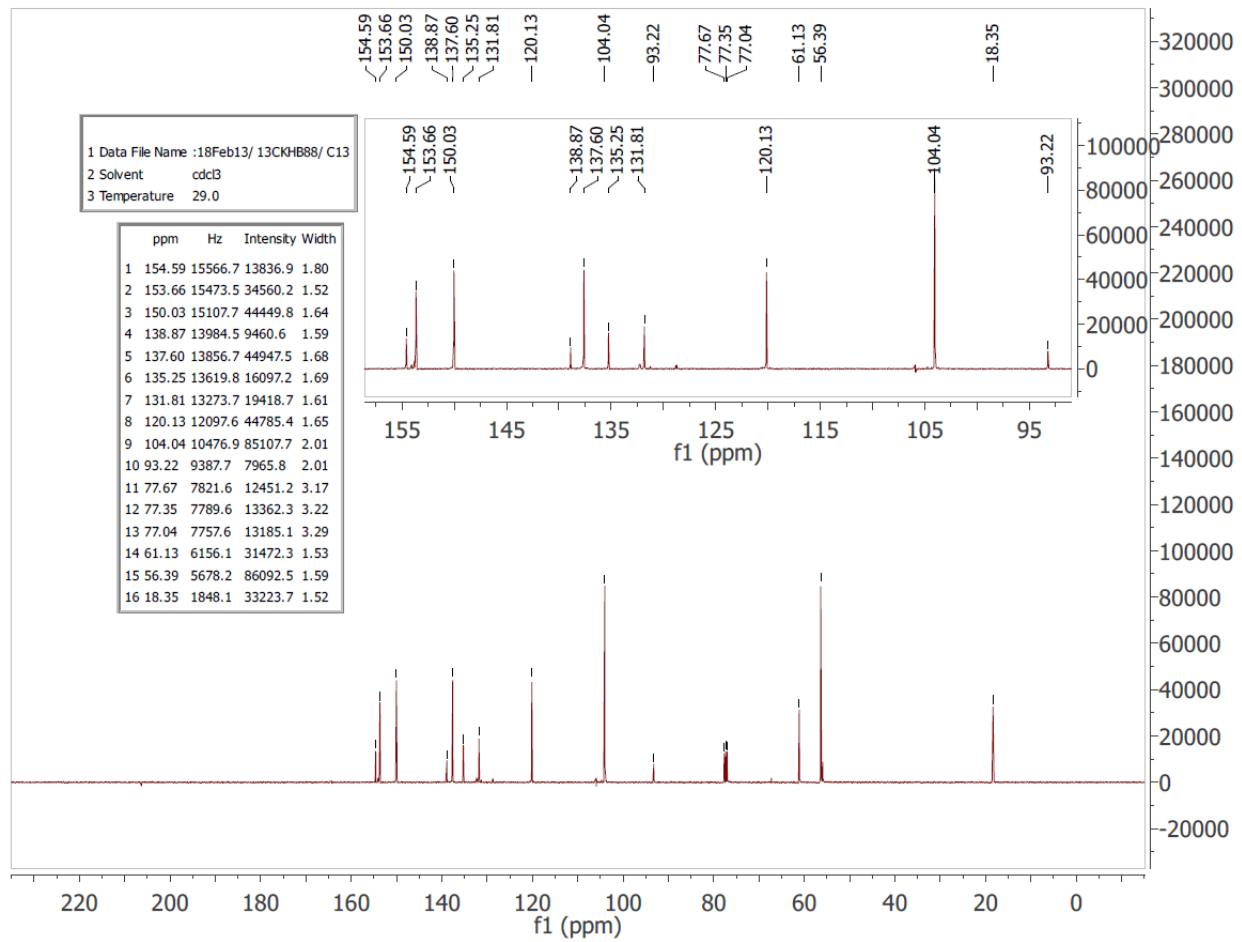


Figure S6. ^{13}C NMR spectrum of 2-(3',4',5'-Trimethoxyphenyl)-5-methylpyridine (3,4,5-tMeOppy) in CDCl_3

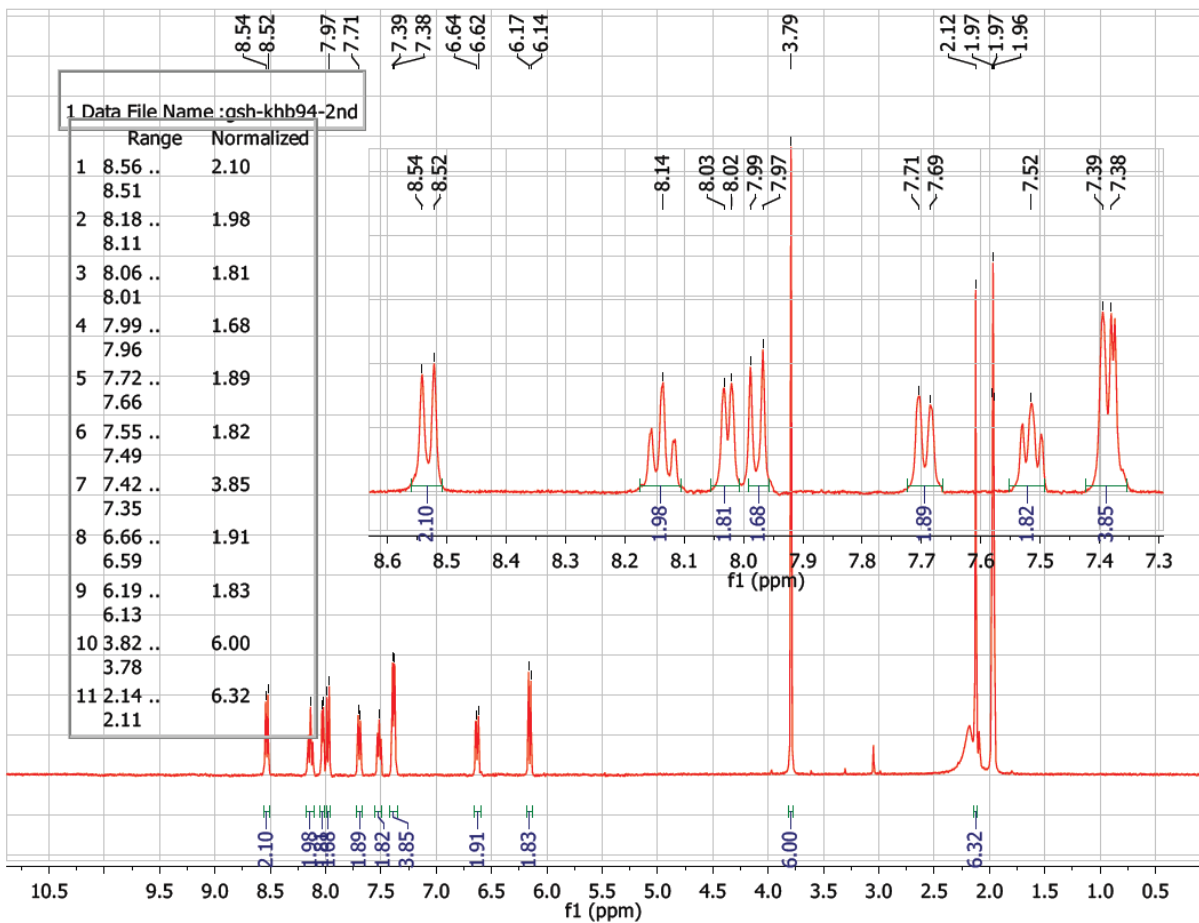


Figure S7. ^1H NMR spectrum of $[\text{Ir}(3\text{-MeOppy})_2(\text{bpy})](\text{PF}_6)$ **1a** in CD_3CN

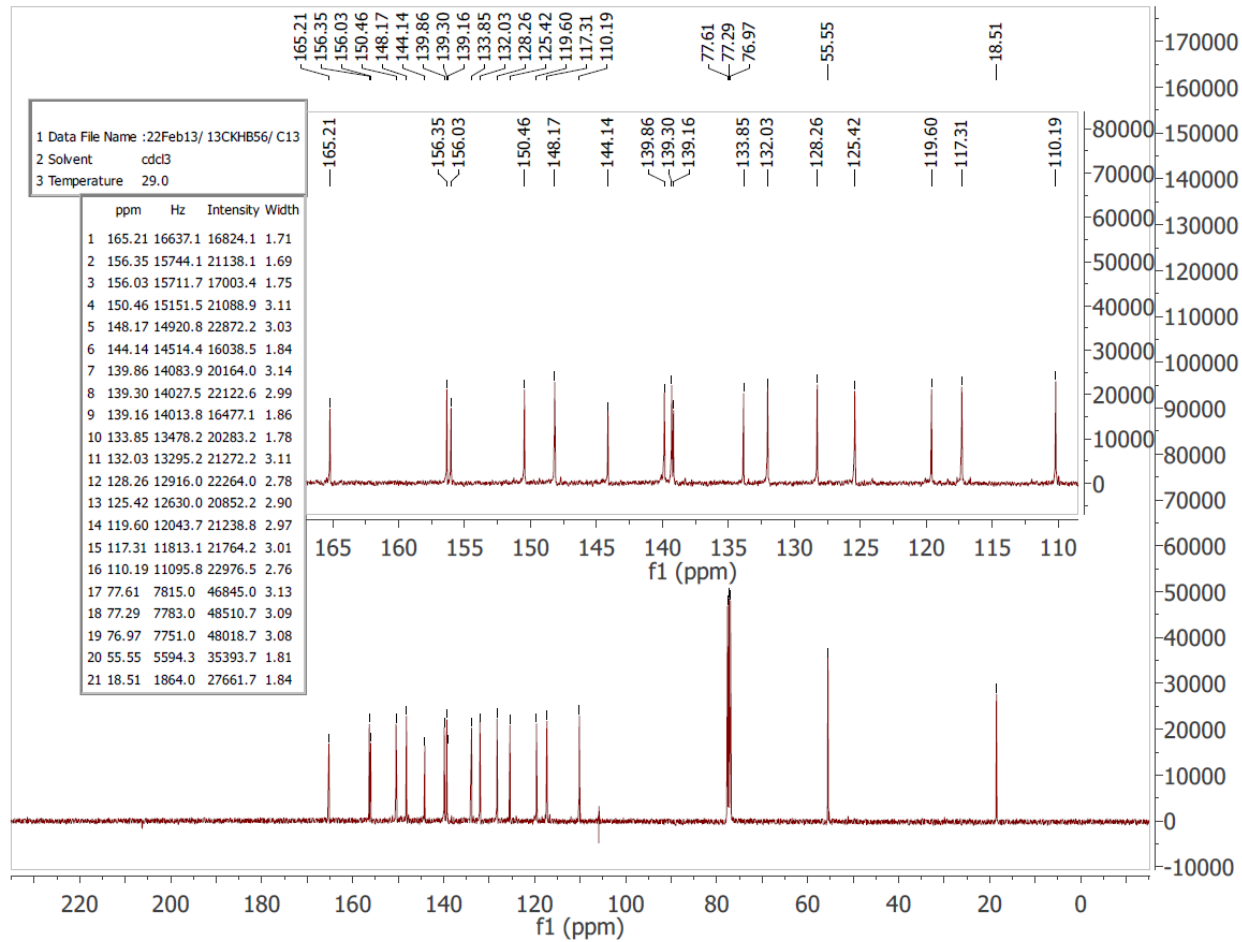


Figure S8. ^{13}C NMR spectrum of $[\text{Ir}(3\text{-MeOppy})_2(\text{bpy})](\text{PF}_6)$ **1a** in CDCl_3

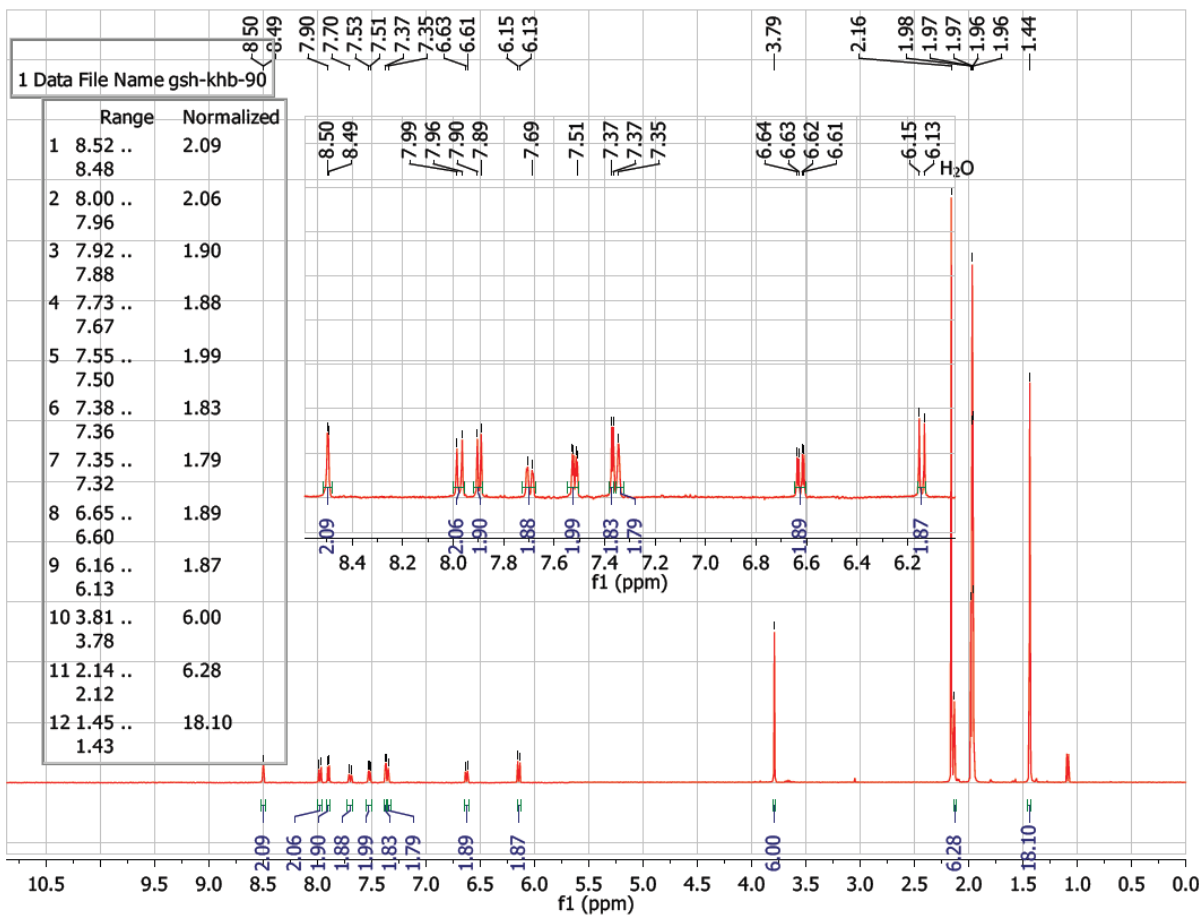


Figure S9. ^1H NMR spectrum of $[\text{Ir}(3\text{-MeO-ppy})_2(\text{dtbbupy})](\text{PF}_6)$ **1b** in CD_3CN

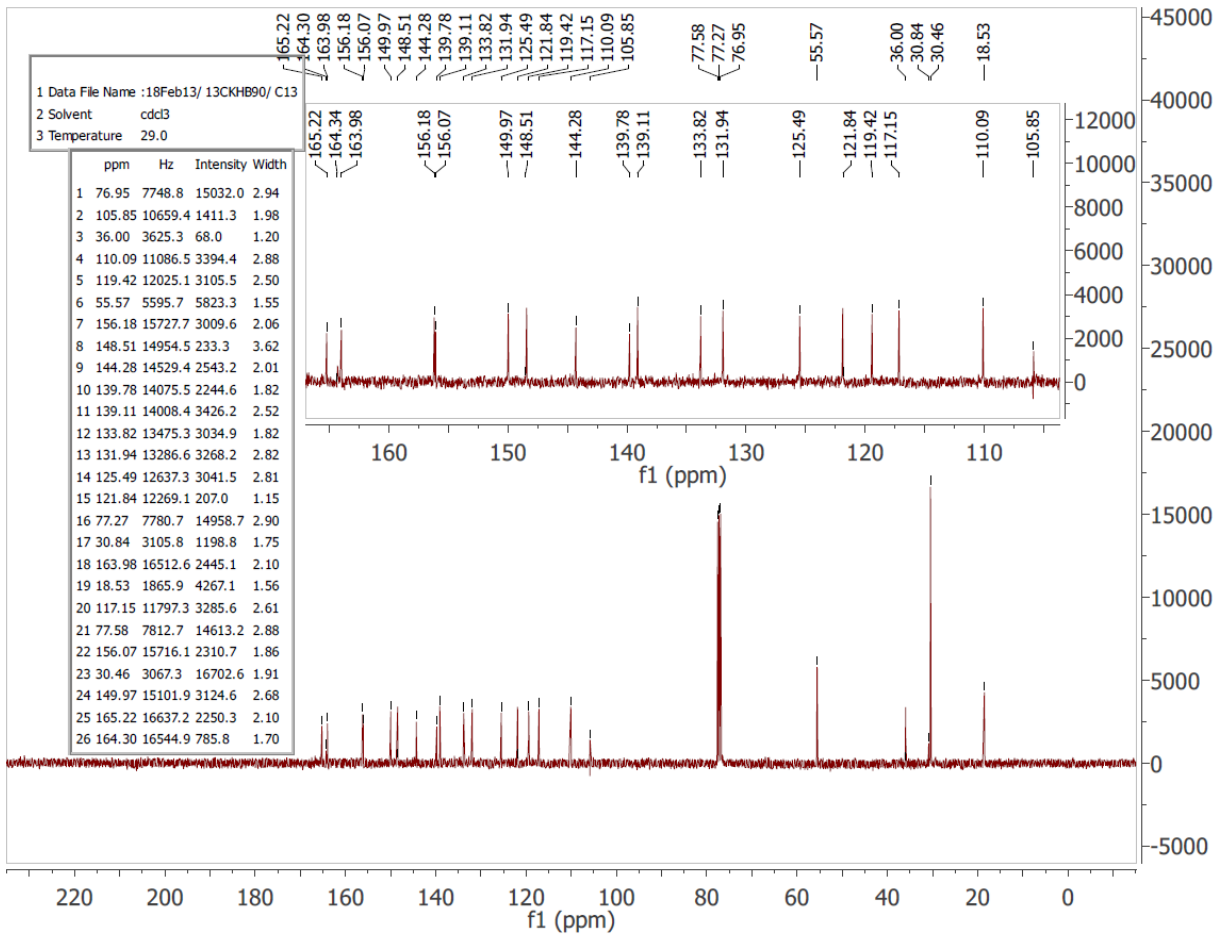


Figure S10. ^{13}C NMR spectrum of $[\text{Ir}(3\text{-MeO-ppy})_2(\text{dtbbpy})](\text{PF}_6)$ **1b** in CDCl_3

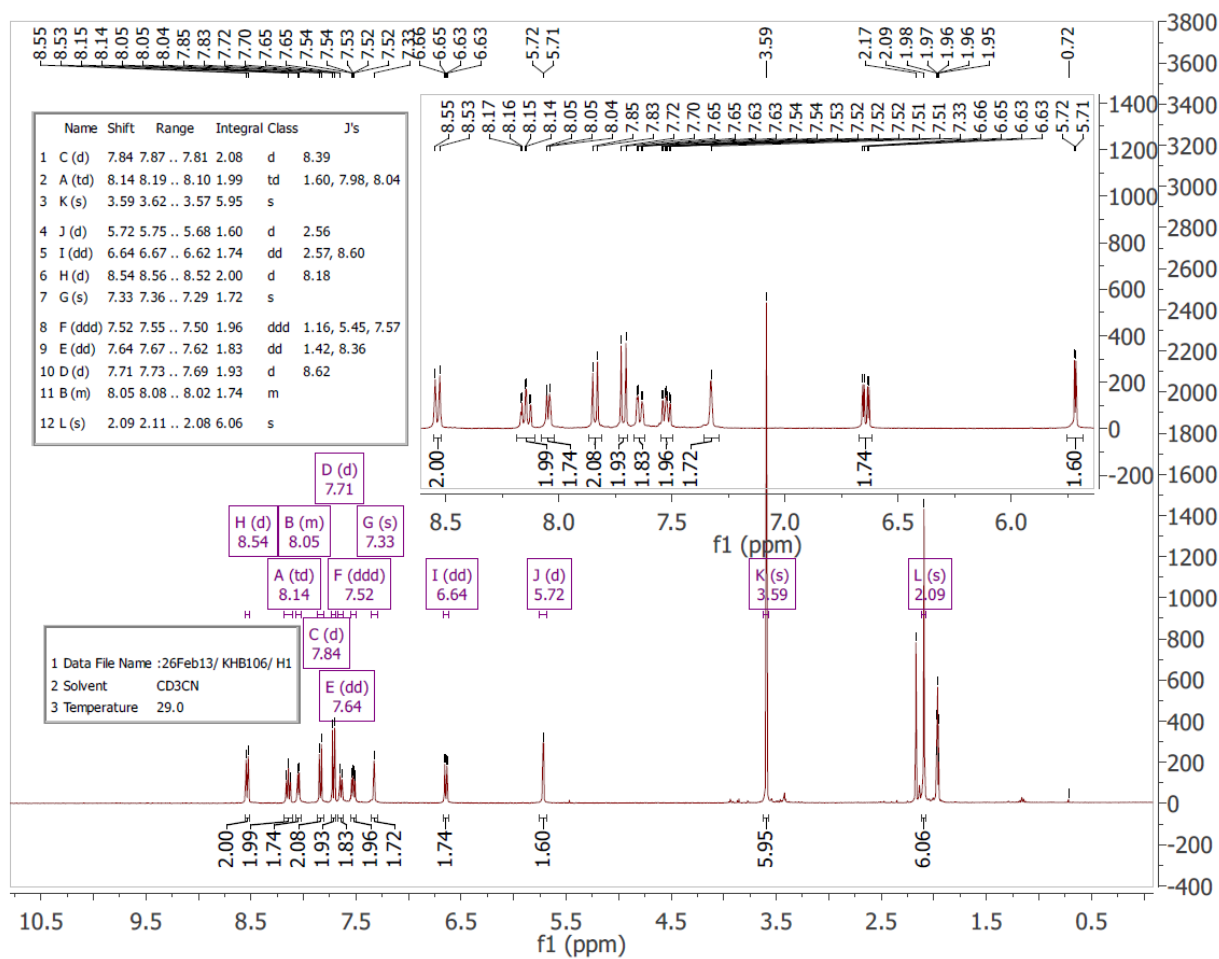


Figure S11. ^1H NMR spectrum of $[\text{Ir}(4\text{-MeOppy})_2(\text{bpy})](\text{PF}_6)$ **2a** in CD₃CN

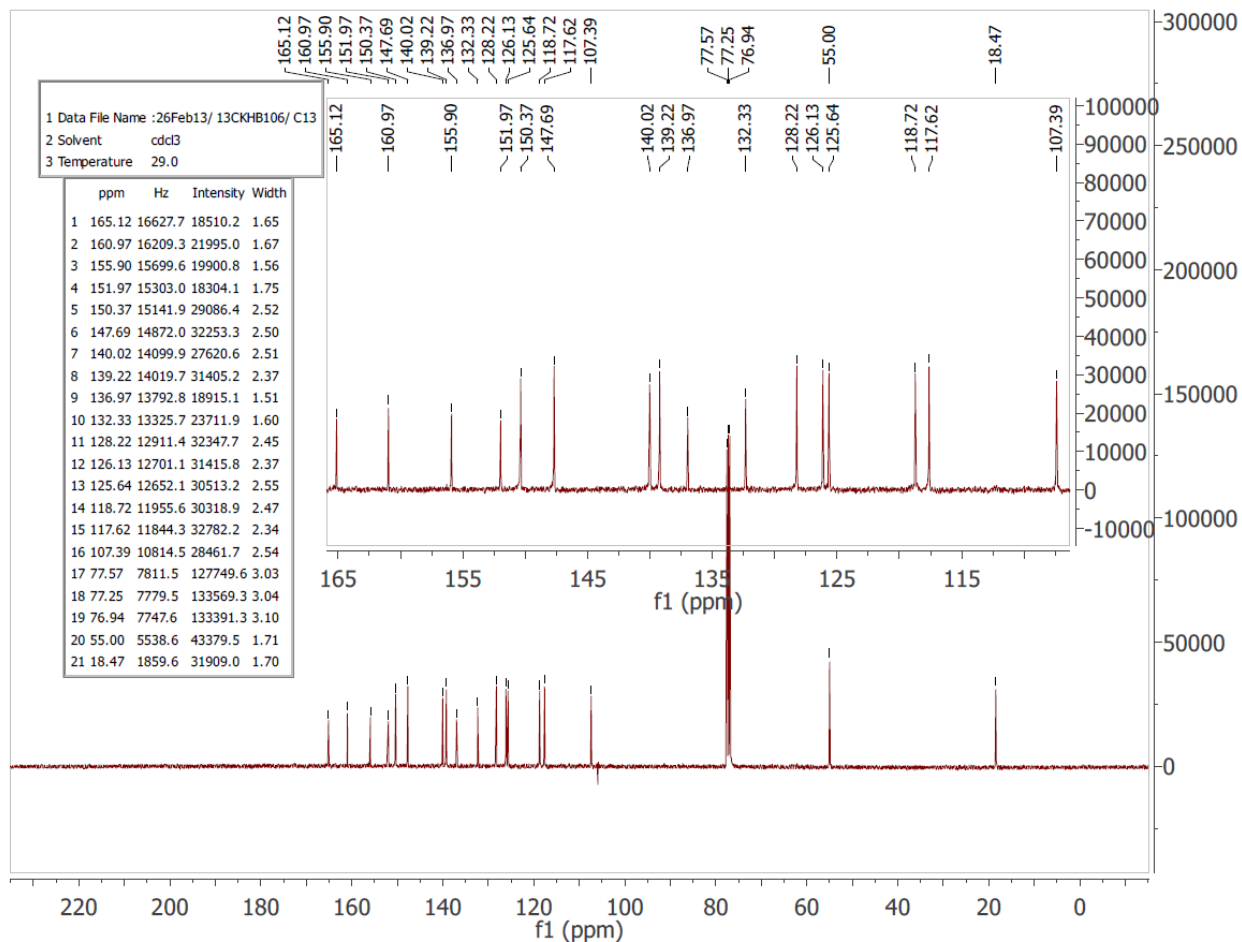


Figure S12. ^{13}C NMR spectrum of $[\text{Ir}(4\text{-MeOppy})_2(\text{bpy})](\text{PF}_6)$ **2a** in CDCl_3

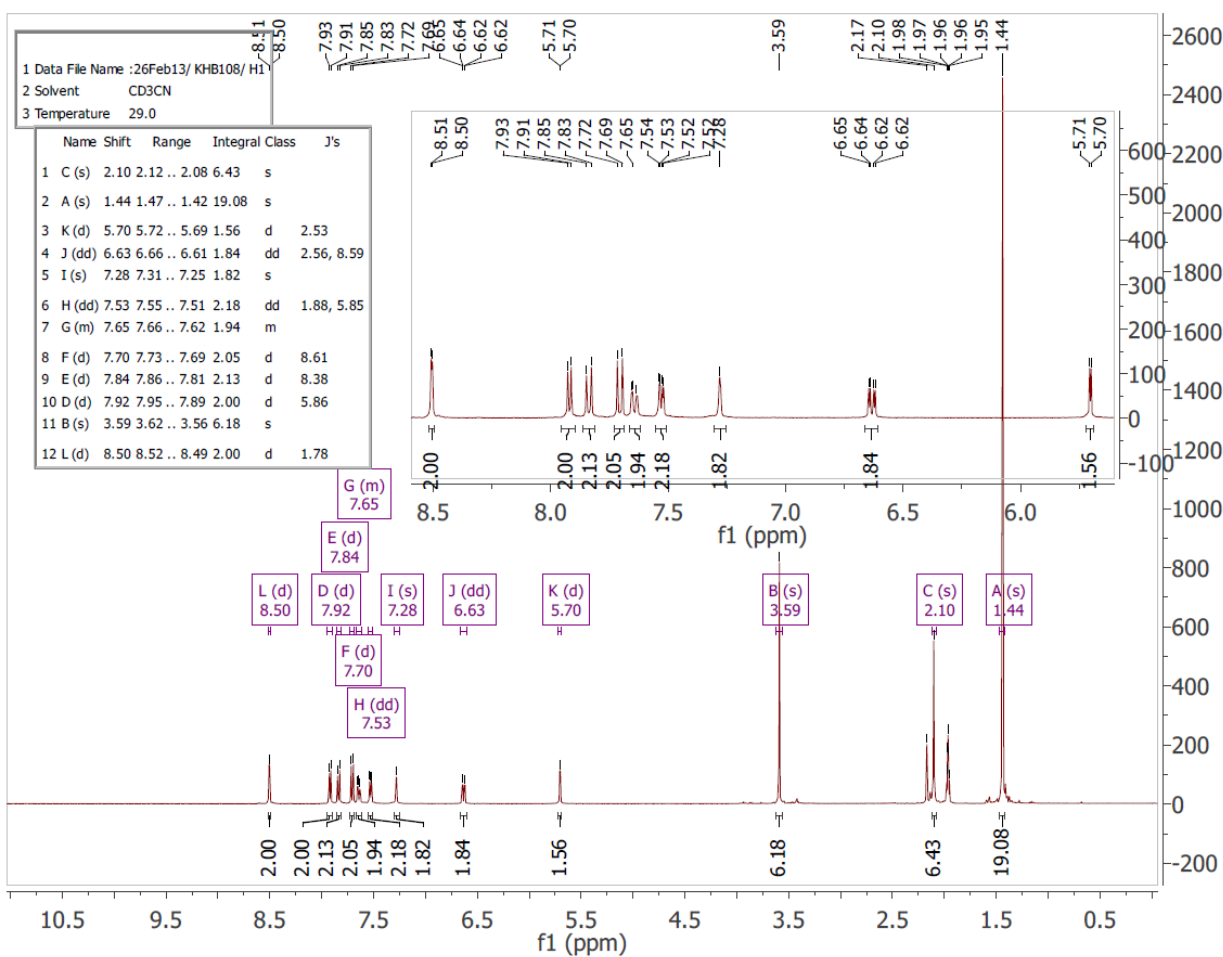


Figure S13. ^1H NMR spectrum of $[\text{Ir}(4\text{-MeOppy})_2(\text{dtbubpy})](\text{PF}_6)$ **2b** in CD_3CN

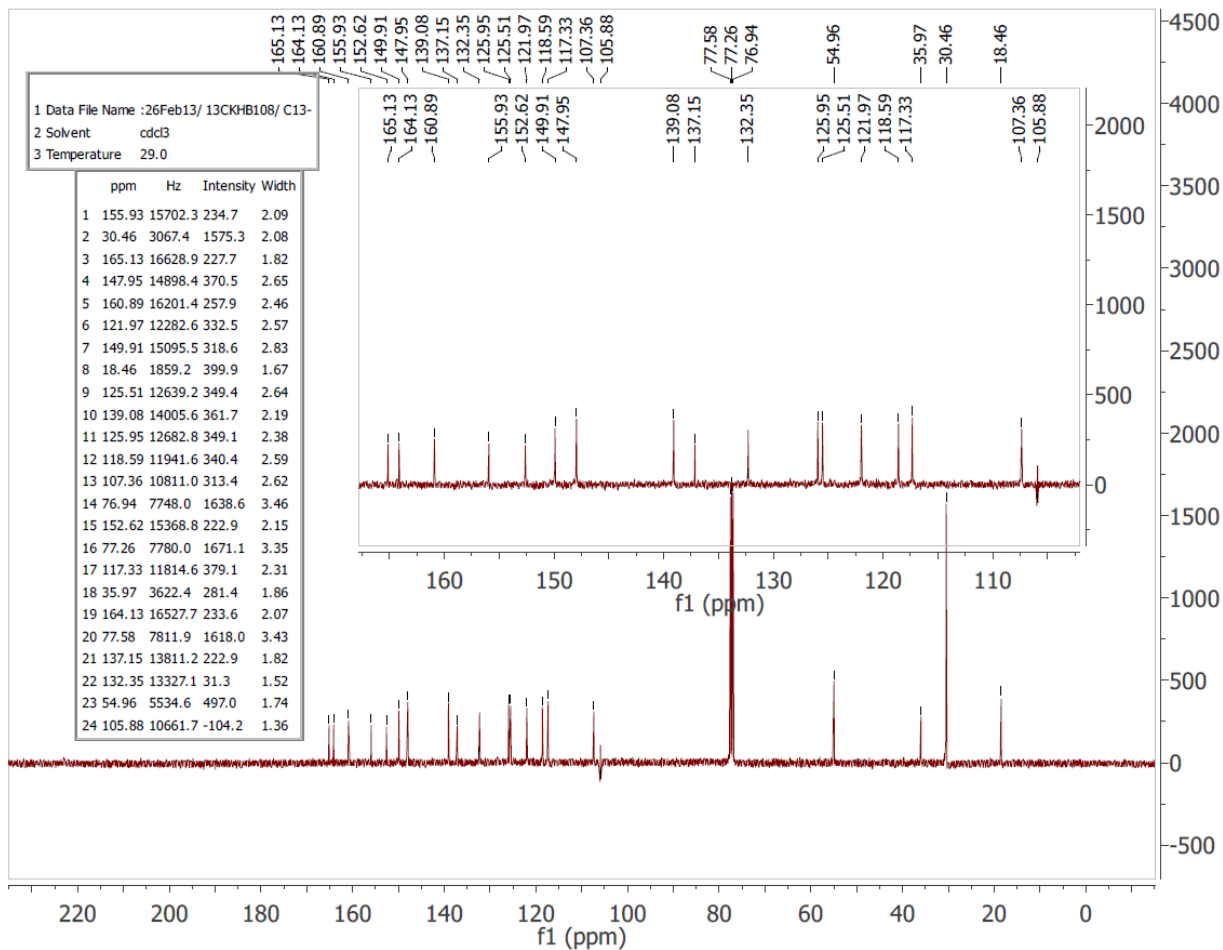


Figure S14. ^{13}C NMR spectrum of $[\text{Ir}(4\text{-MeOppy})_2(\text{dtbbupy})](\text{PF}_6)$ **2b** in CDCl_3

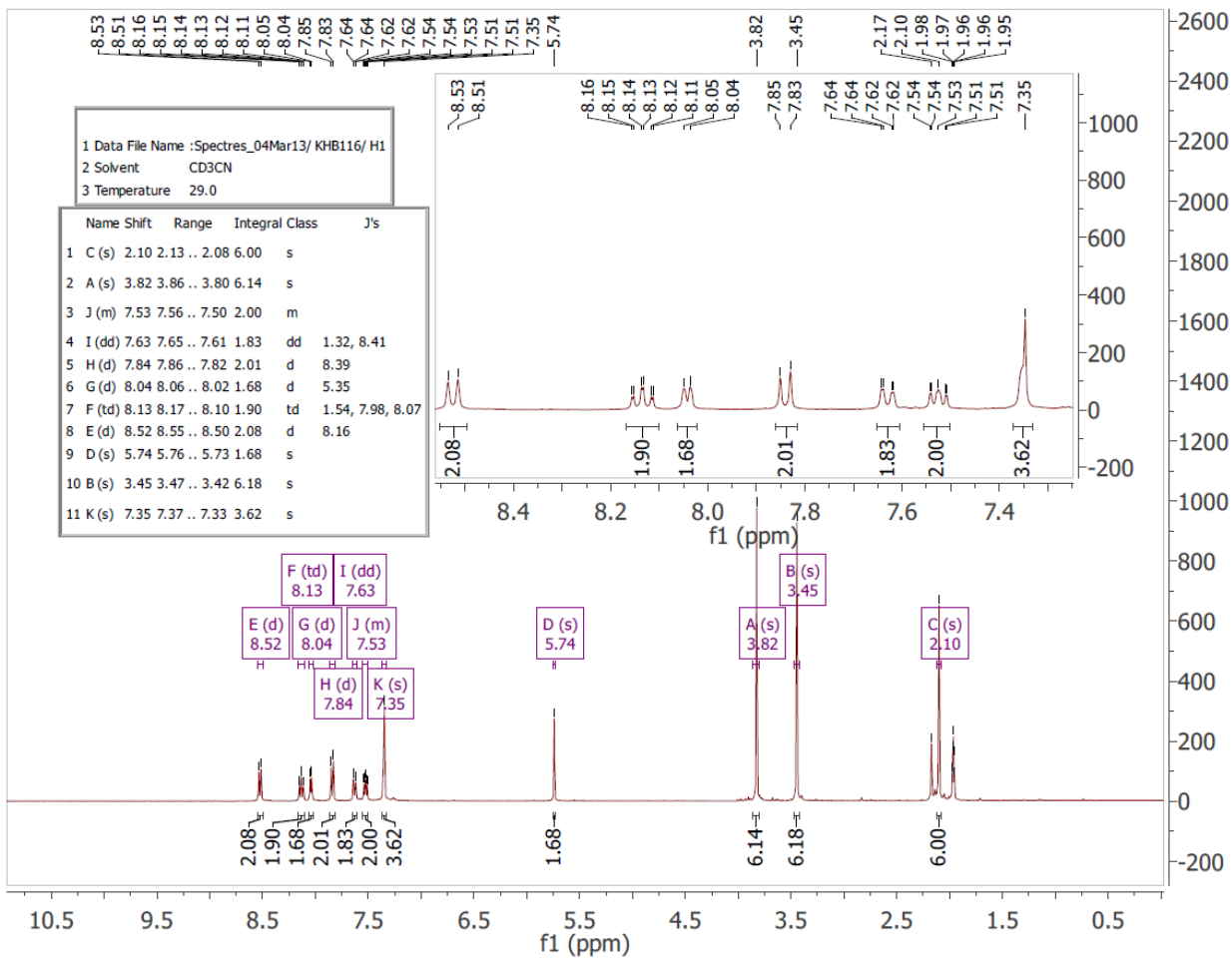


Figure S15. ¹H NMR spectrum of [Ir(3,4-dMeOppy)₂(bpy)](PF₆) 3a in CD₃CN

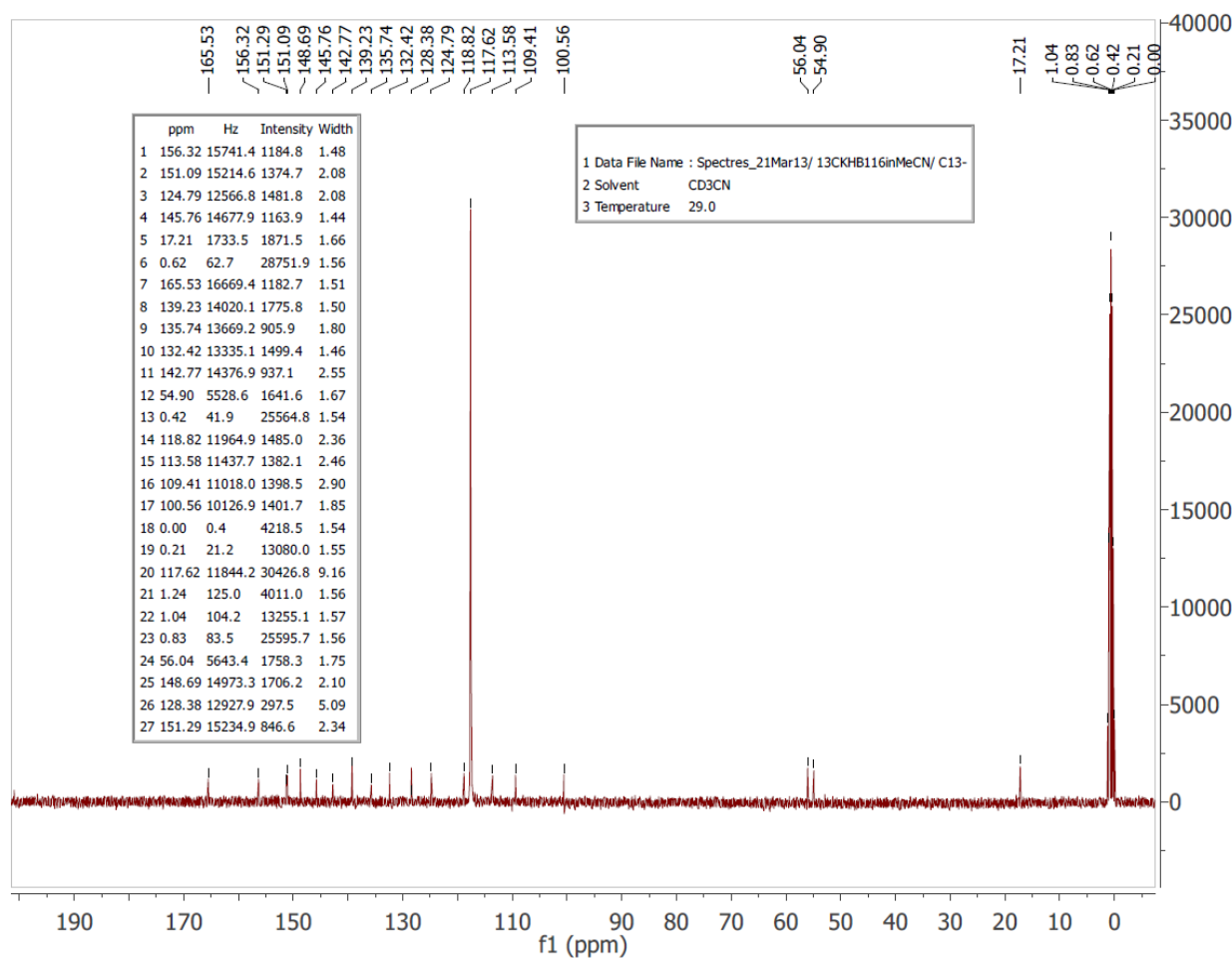


Figure S16. ^{13}C NMR spectrum of $[\text{Ir}(3,4\text{-dMeOppy})_2(\text{bpy})](\text{PF}_6)$ 3a in CD_3CN

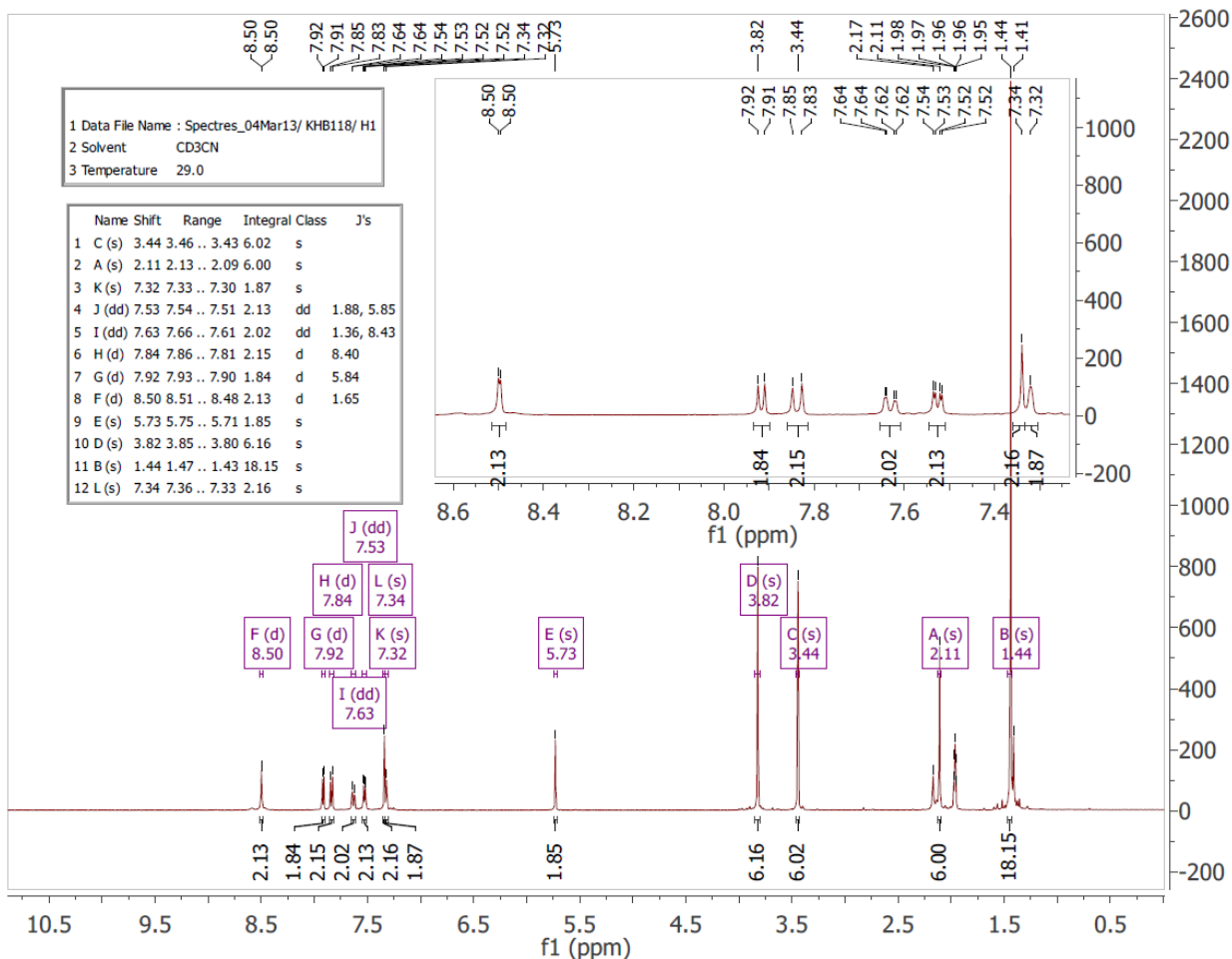


Figure S17. ^1H NMR spectrum of $[\text{Ir}(3,4\text{-dMeOppy})_2(\text{dtbubpy})](\text{PF}_6)$ 3b in CD_3CN

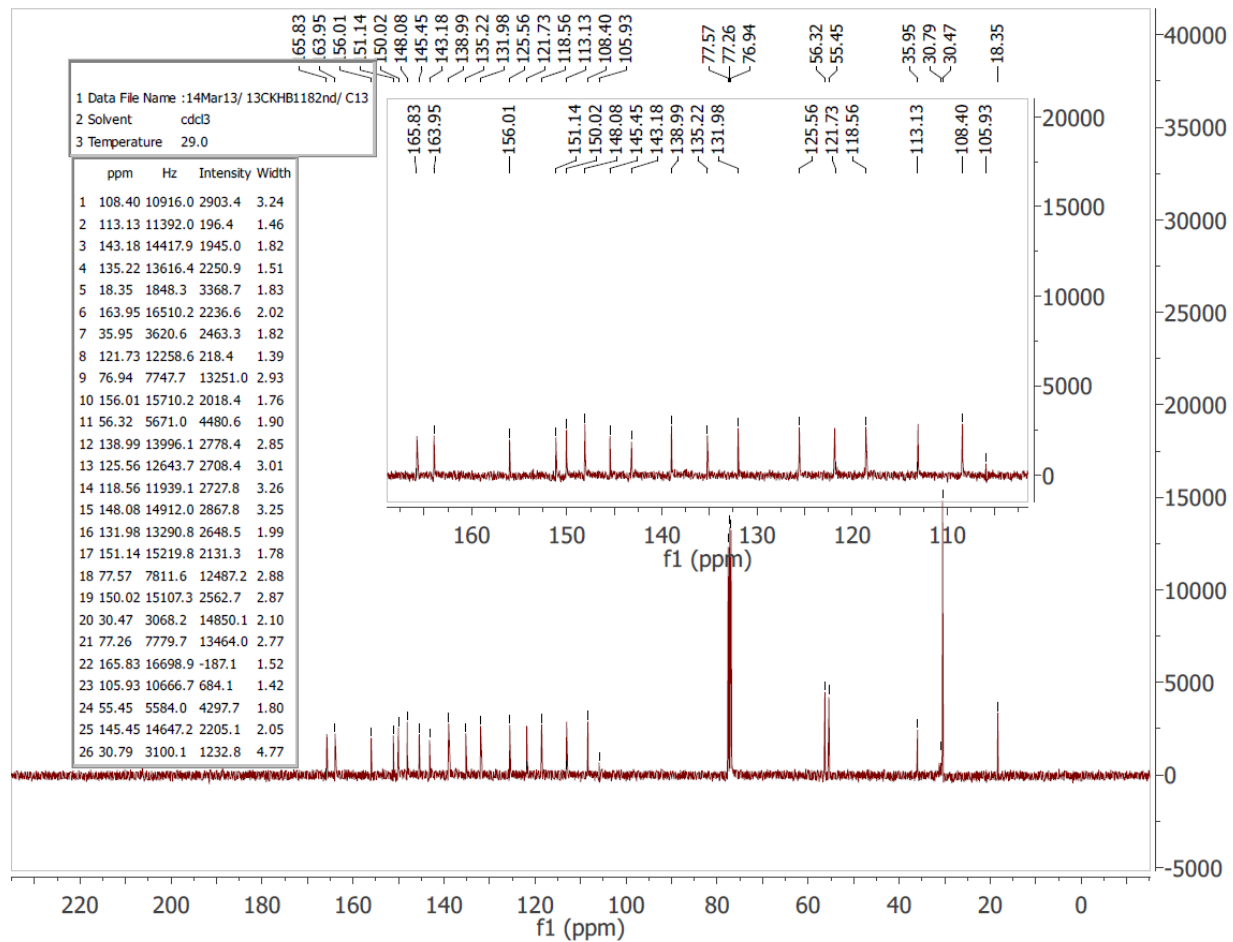


Figure S18. ¹³C NMR spectrum of [Ir(3,4-dMeOppy)₂(dtbbpy)](PF₆) **3b** in CDCl₃

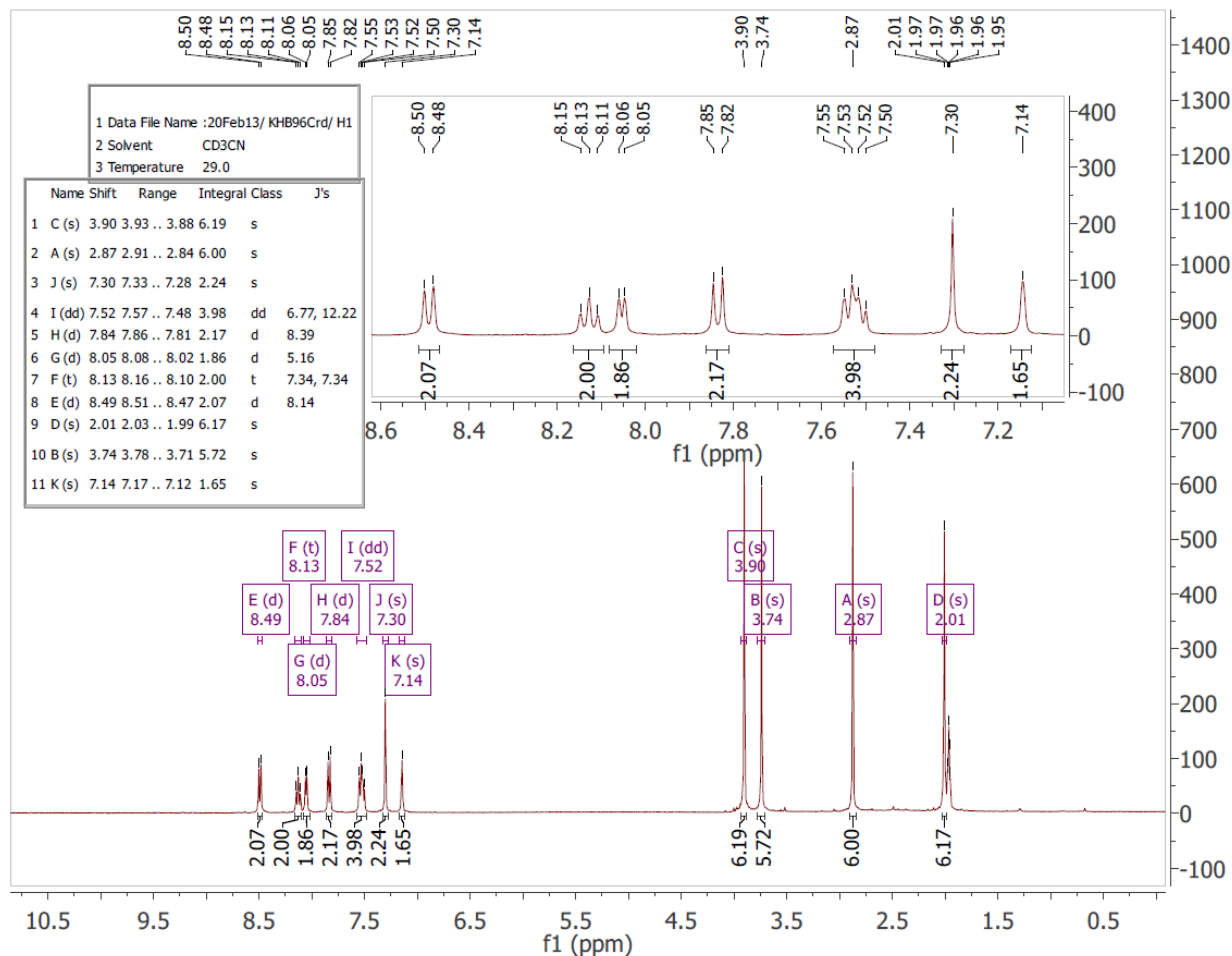


Figure S19. ¹H NMR spectrum of [Ir(3,4,5-tMeOppy)₂(bpy)](PF₆) 4a in CD₃CN

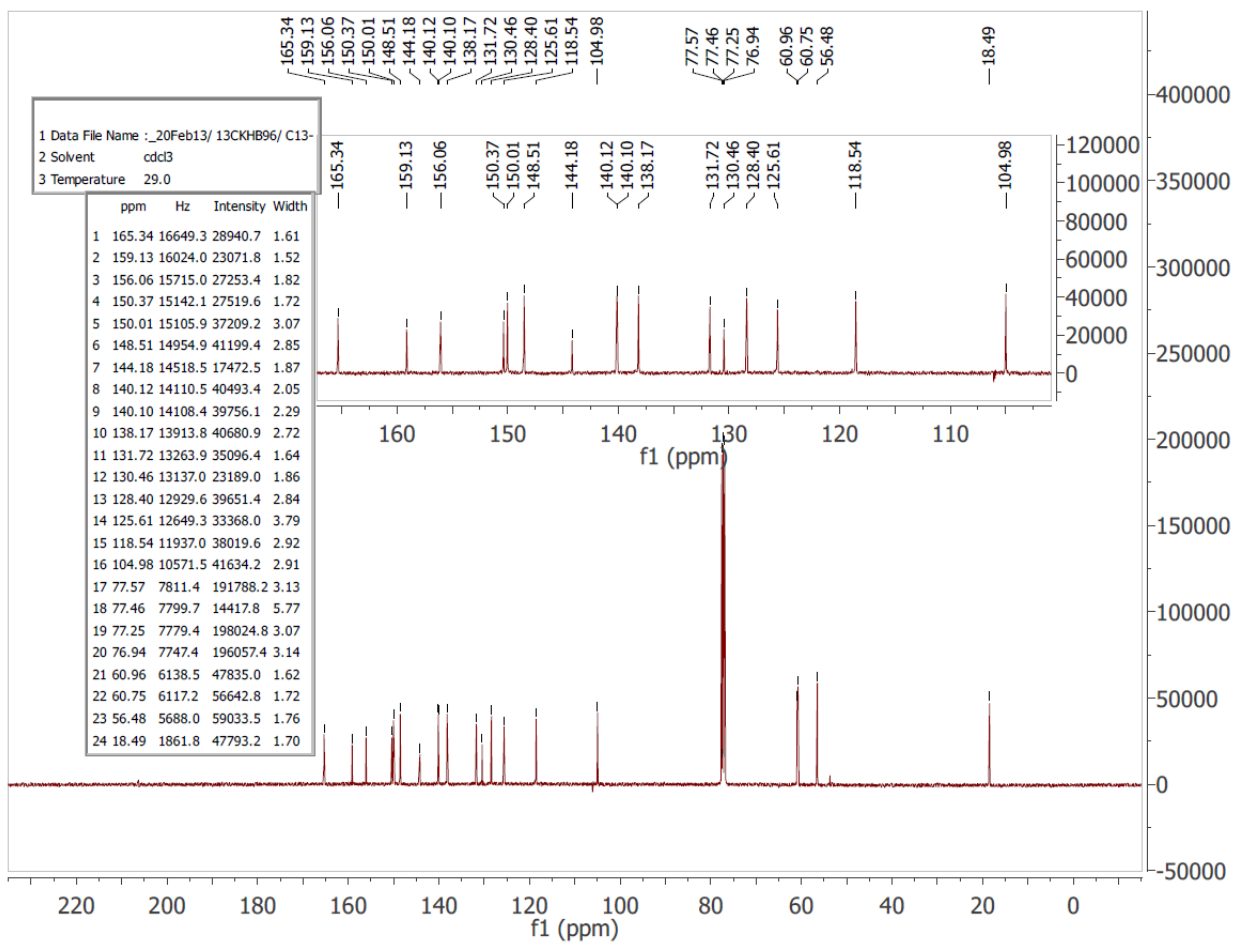


Figure S20. ^{13}C NMR spectrum of $[\text{Ir}(3,4,5\text{-tMeOppy})_2(\text{bpy})](\text{PF}_6)$ **4a** in CDCl_3

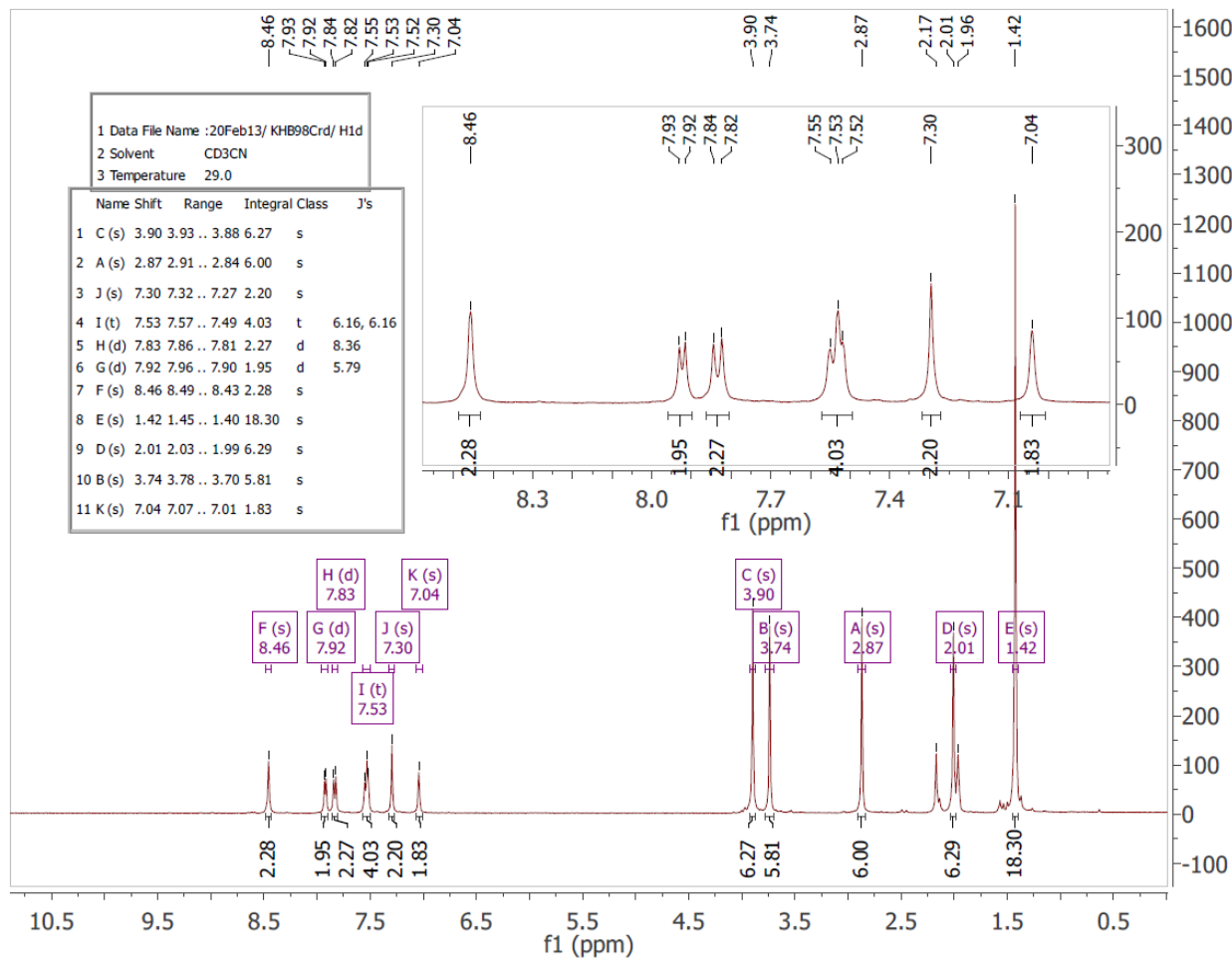


Figure S21. ¹H NMR spectrum of [Ir(3,4,5-tMeOppy)₂(dtbbupy)](PF₆) **4b** in CD₃CN

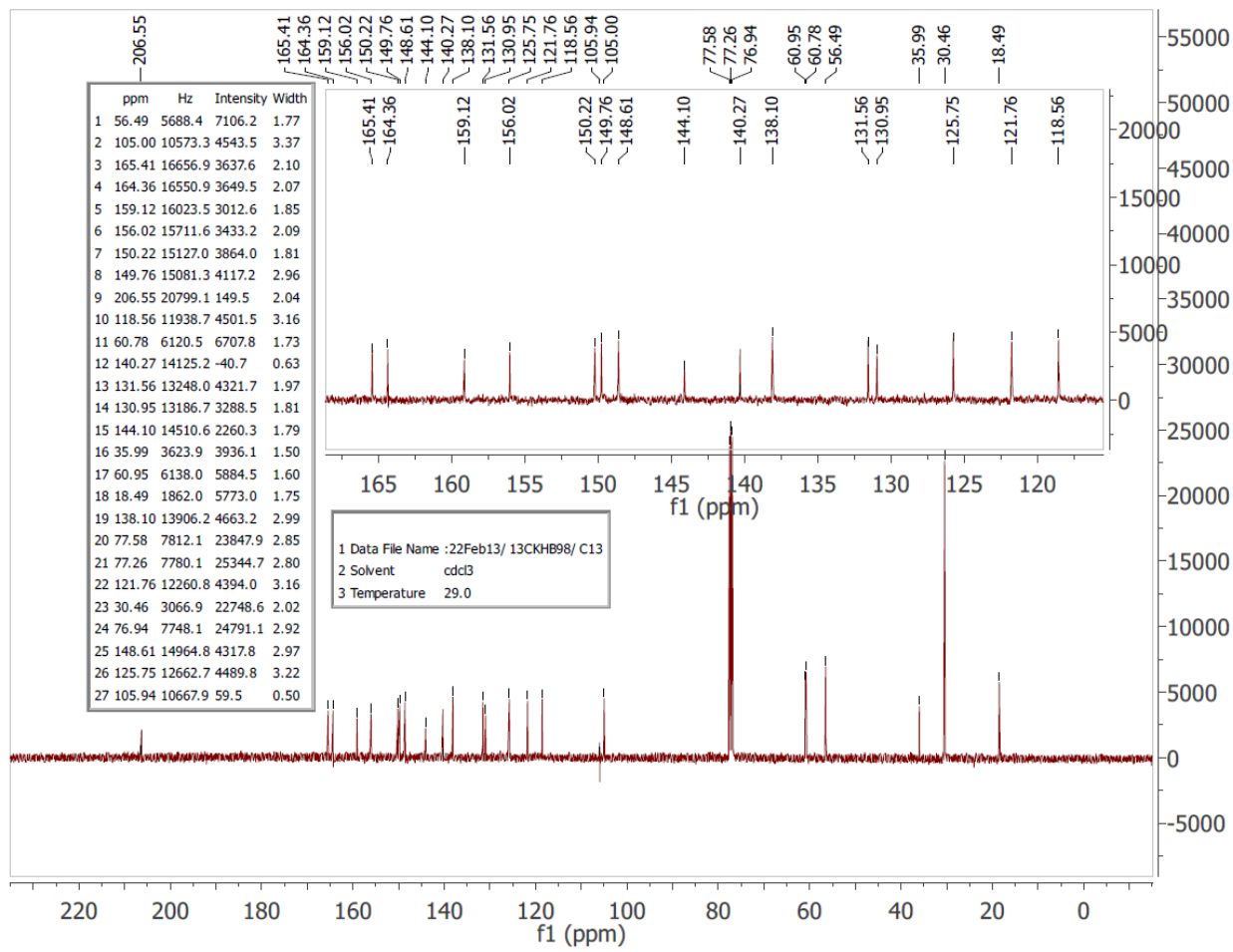


Figure S22. ^{13}C NMR spectrum of $[\text{Ir}(3,4,5\text{-tMeOppy})_2(\text{dtbbupy})](\text{PF}_6)$ **4b** in CDCl_3

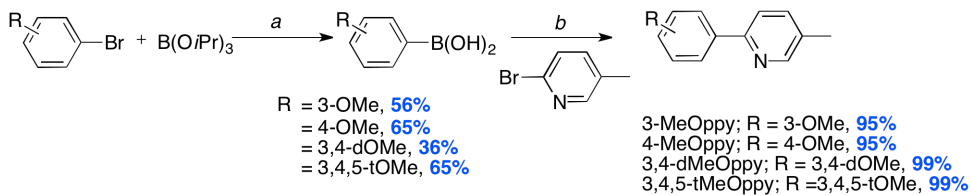


Figure S23. Synthesis of C^N ligands. Reagents and conditions: ^a i. toluene/THF (4:1 v/v), 1.2 equiv. *n*-BuLi, -78 °C, N₂; ii. 1 N HCl, -20 °C, RT, 0.5 h. ^b 1,4-dioxane/H₂O (4:1 v/v), 3.0 equiv. K₂CO₃, 5 mol% Pd(PPh₃)₄, N₂, 105 °C, 19 h.

Table S1. Relevant electrochemical data for complexes **1a-4b**.^a

complex	ligands		<i>E</i> _{1/2,OX} V	<i>ΔE</i> _p mV	<i>E</i> _{1/2,red} V	<i>ΔE</i> _p mV	<i>ΔE</i> V
	C ^N	N ^N					
1a	3-MeOppy	bpy	0.95	76	-1.40	69	2.38
1b	3-MeOppy	d/B bpy	0.90	75	-1.52	70	2.49
2a	4-MeOppy	bpy	1.15 ^b	-	-1.42	70	2.61
2b	4-MeOppy	d/B bpy	1.13 ^b	-	-1.49	70	2.63
3a	3,4-dMeOppy	bpy	0.84	75	-1.41	71	2.27
3b	3,4-dMeOppy	d/B bpy	0.78	69	-1.52	67	2.35
4a	3,4,5-tMeOppy	bpy	0.87	75	-1.40	74	2.30
4b	3,4,5-tMeOppy	d/B bpy	0.84	76	-1.50	70	2.42

^aCV traces recorded in MeCN solution with 0.1 M (*n*-Bu₄N)PF₆ at 298 K at 50 mVs⁻¹. Values are in V vs. SCE (Fc/Fc⁺ vs. SCE = 0.38 V).¹ A non-aqueous Ag/Ag⁺ electrode (silver wire in a solution of 0.1 M AgNO₃ in MeCN) was used as the pseudoreference electrode; a glassy-carbon electrode was used for the working electrode and a Pt electrode was used as the counter electrode. ^b Irreversible and *E*_{pa} reported for oxidation peak potentials.

Table S2. Relevant spectroscopic data for complex **1a-4b**.

Complex	$\lambda_{\text{abs}} / \text{nm} (\epsilon / 10^4 \text{ M}^{-1} \text{ cm}^{-1})^a$	$E_{0,0} (\text{nm})$
1a	265 (8.37), 311 (3.14), 338 (1.61), 425 (0.70)	498
1b	263 (10.61), 308 (4.18), 338 (2.09), 425(0.80)	492
2a	255 (5.32), 277 (6.78), 309 (3.71), 390 (0.86), 450* (0.11)	464
2b	250 (6.62), 278 (8.88), 310 (3.75), 390 (0.82), 450* (0.09)	471
3a	279 (5.72), 308 (2.47), 340 (1.57), 419 (0.74)	472
3b	279 (6.76), 312 (2.75), 343 (1.78), 424 (0.78)	480
4a	244 (6.22), 275 (6.68), 310 (4.21), 330 (2.72), 385 (0.93)	460
4b	248 (8.81), 275 (9.45), 310 (5.89), 331 (3.76), 395 (1.14)	473

^a Absorption spectra recorded in aerated MeCN at 298 K. Molar absorptivities (ϵ) determined over a concentration range of 6.88×10^{-1} to $3.19 \times 10^2 \mu\text{M}$ wherein absorbance values obey the Beer-Lambert law. ^b $E_{0,0}$ was estimated from the onset of the absorption spectrum at approximately 10% intensity. * Shoulder.

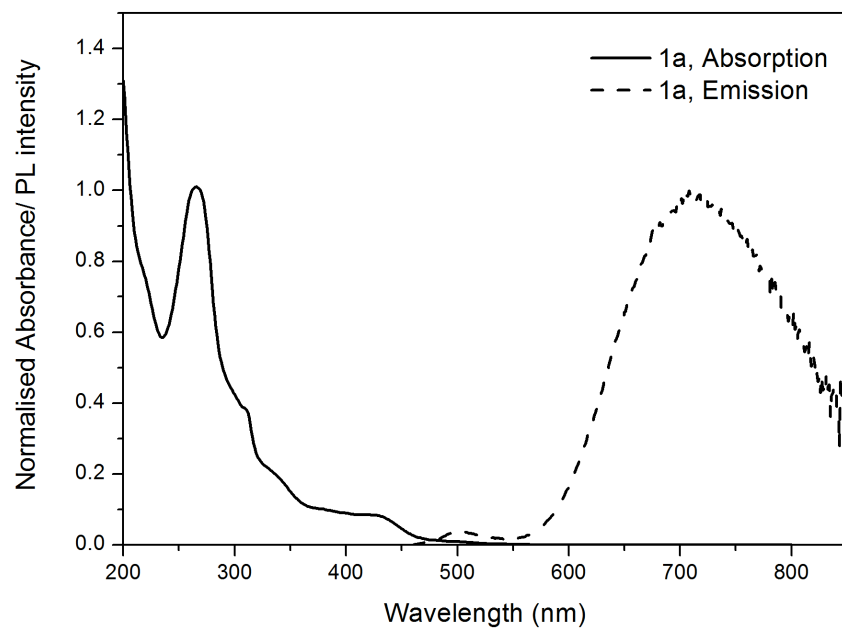


Figure S23. Normalized absorption and emission spectra of $[\text{Ir}(3\text{-MeOppy})_2(\text{bpy})](\text{PF}_6)$ **1a** recorded in MeCN at 298 K

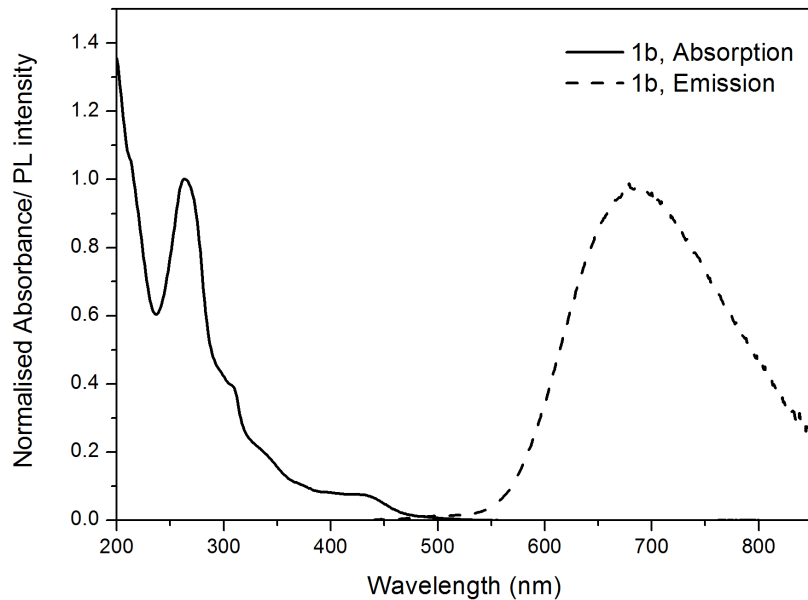


Figure S24. Normalized absorption and emission spectra of $[\text{Ir}(3\text{-MeO-ppy})_2(\text{dtbbpy})](\text{PF}_6)$ **1b** recorded in MeCN at 298 K

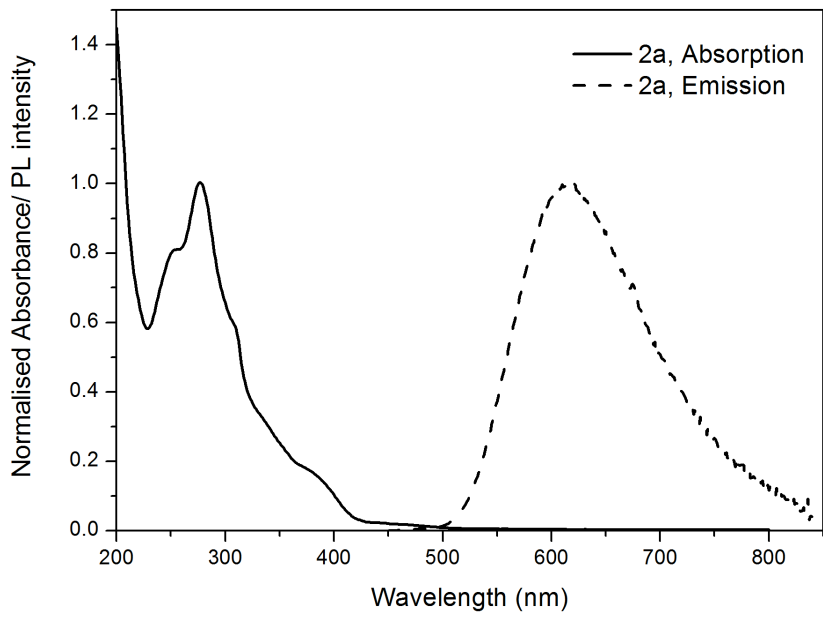


Figure S25. Normalized absorption and emission spectra of $[\text{Ir}(4\text{-MeOppy})_2(\text{bpy})](\text{PF}_6)$ **2a** recorded in MeCN at 298 K

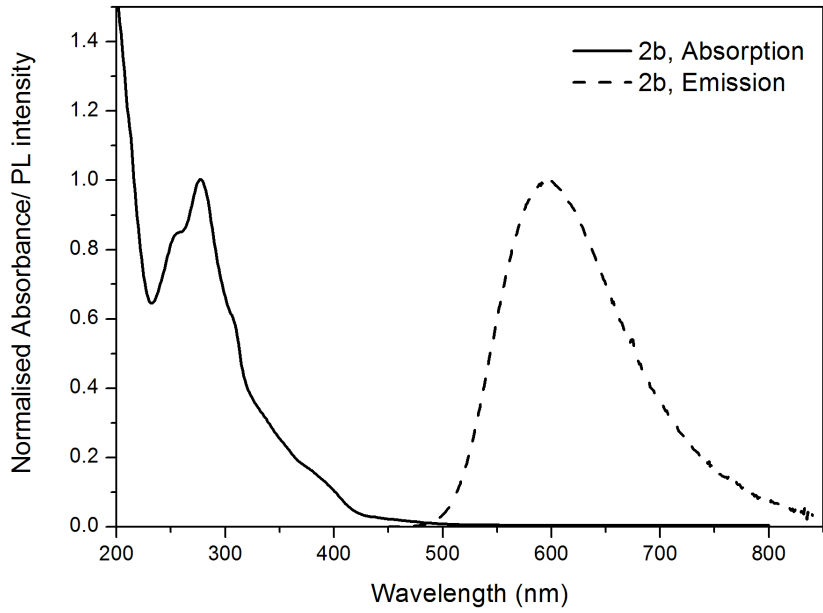


Figure S26. Normalized absorption and emission spectra of $[\text{Ir}(4\text{-MeOppy})_2(\text{dtbbpy})](\text{PF}_6)$ **2b** recorded in MeCN at 298

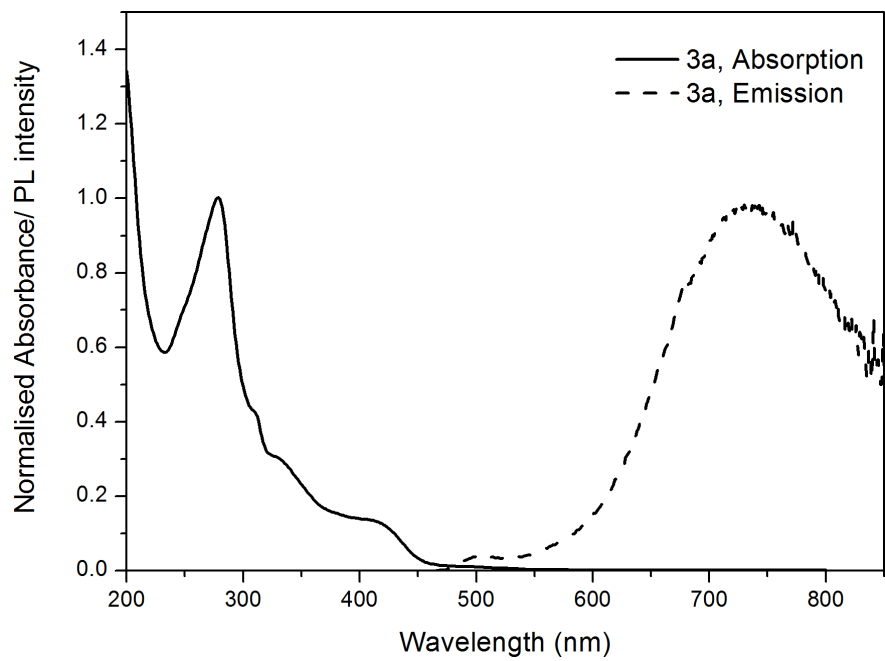


Figure S27. Normalized absorption and emission spectra of $[\text{Ir}(3,4\text{-dMeOppy})_2(\text{bpy})](\text{PF}_6)$ **3a** recorded in MeCN at 298 K

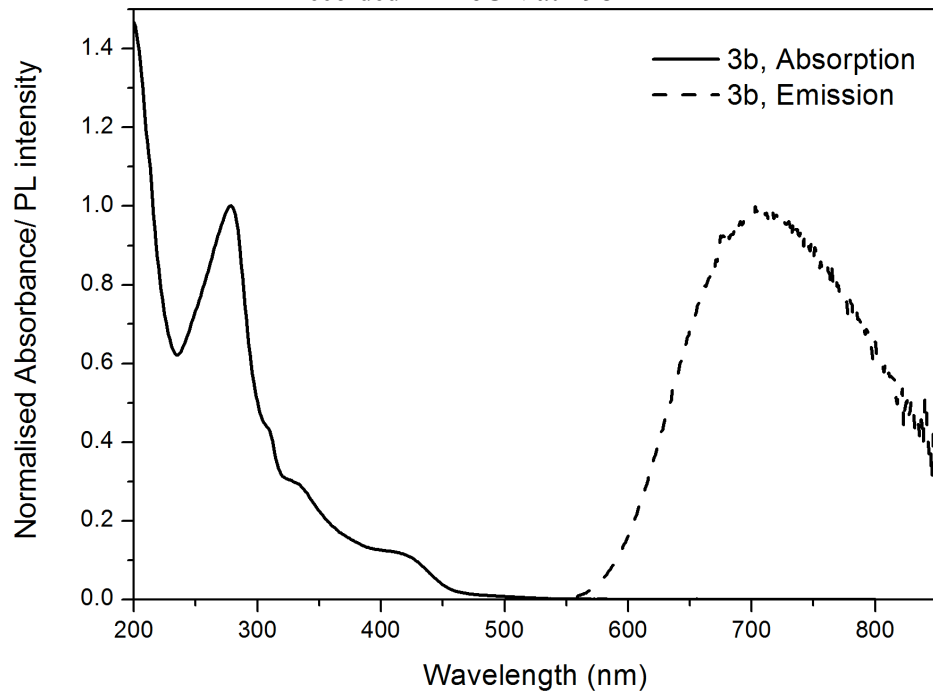


Figure S28. Normalized absorption and emission spectra $[\text{Ir}(3,4\text{-dMeOppy})_2(\text{dtbbpy})](\text{PF}_6)$ **3b** recorded in MeCN at 298 K

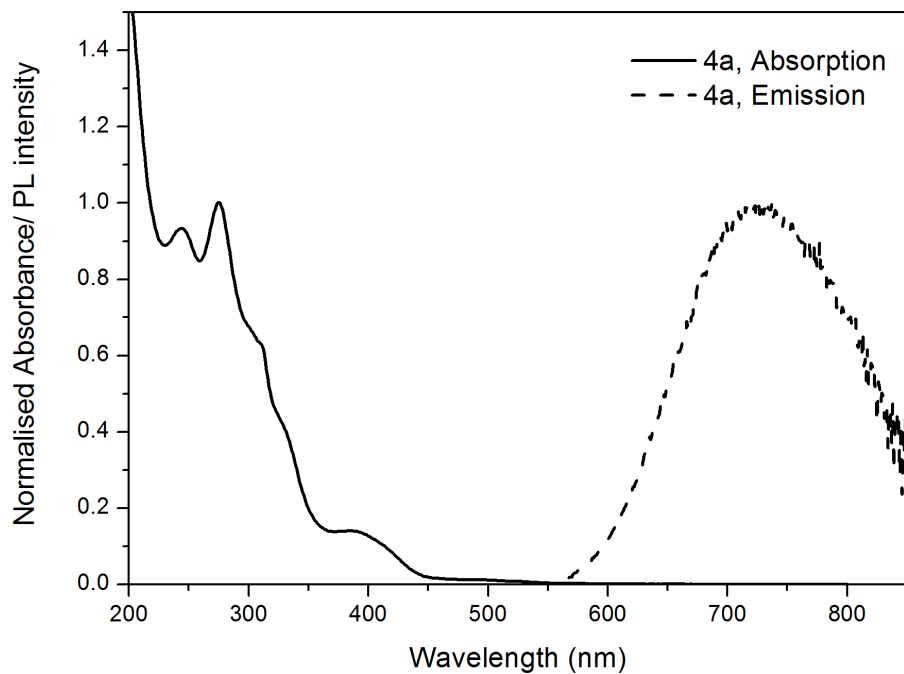


Figure S29. Normalized absorption and emission spectra of $[\text{Ir}(3,4,5\text{-tMeOppy})_2(\text{bpy})](\text{PF}_6)$ **4a** recorded in MeCN at 298 K

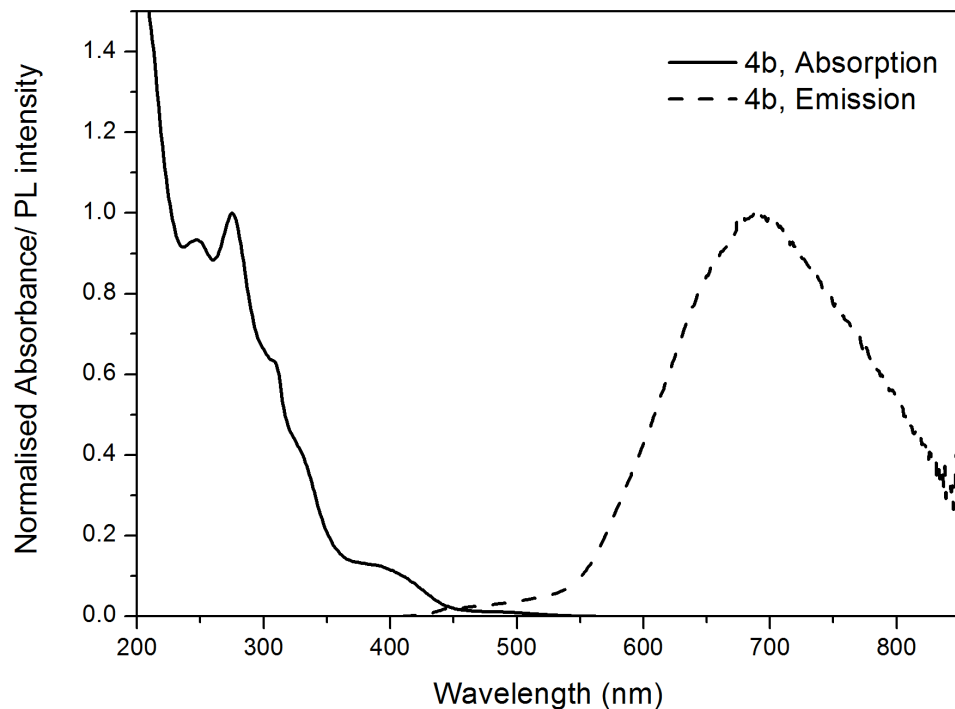


Figure S30. Normalized absorption and emission spectra of $[\text{Ir}(3,4,5\text{-tMeOppy})_2(\text{dtbbpy})](\text{PF}_6)$ **4b** recorded in MECN at 298 K

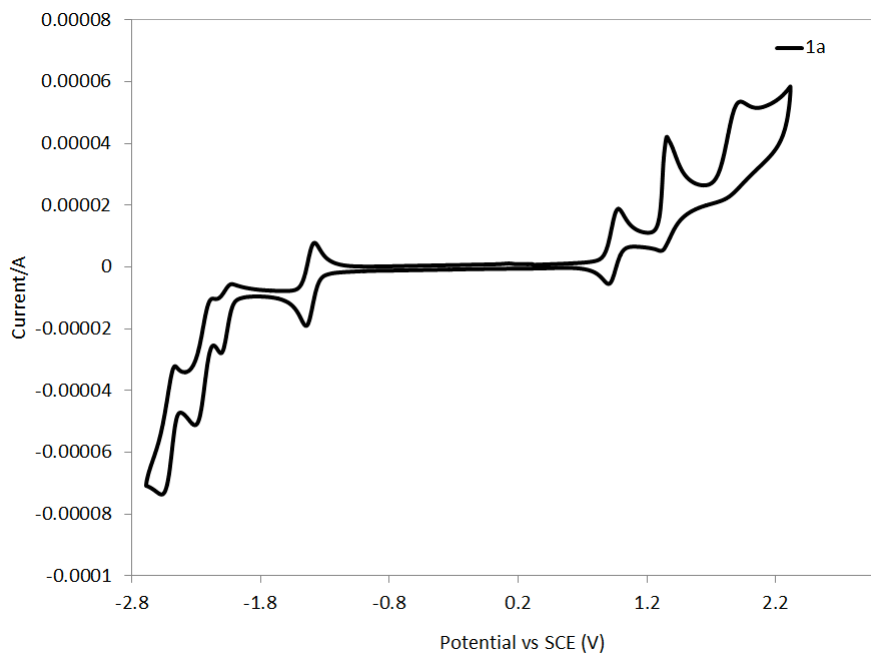


Figure S31. Cyclic voltammogram of $[\text{Ir}(3\text{-MeOppy})_2(\text{bpy})](\text{PF}_6)$ **1a** recorded at 298 K at 50 mV/s in MeCN with 0.1 M ($n\text{Bu}_4\text{N}$) PF_6

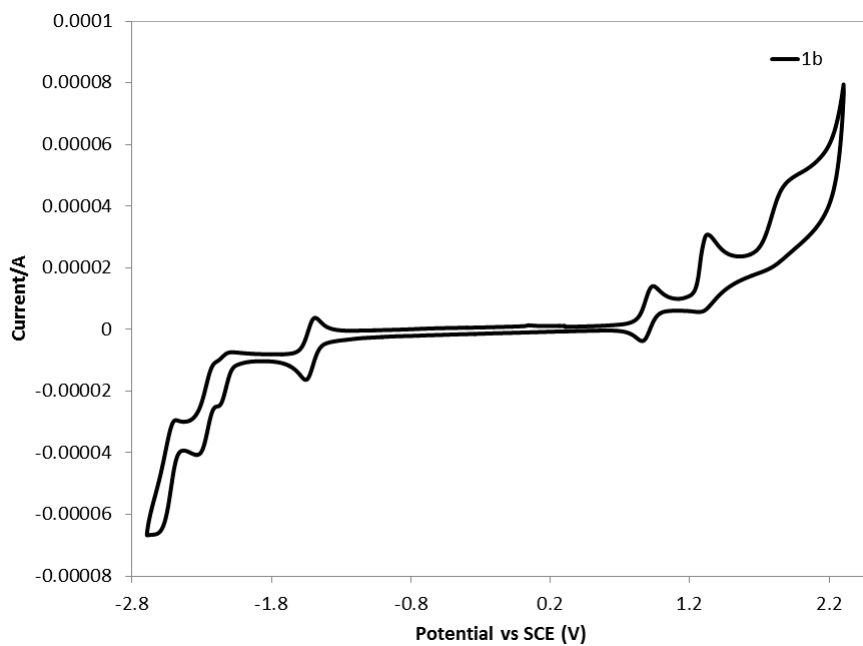


Figure S32. Cyclic voltammogram of $[\text{Ir}(3\text{-MeO-ppy})_2(\text{dtbbpy})](\text{PF}_6)$ **1b** recorded at 298 K at 50 mV/s in MeCN with 0.1 M ($n\text{Bu}_4\text{N}$) PF_6

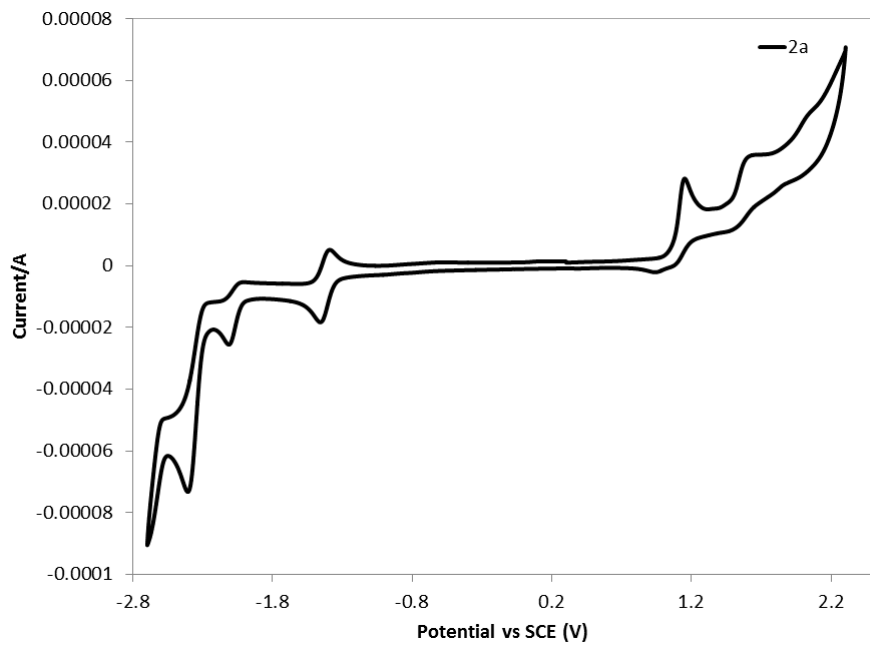


Figure S33. Cyclic voltammogram of $[\text{Ir}(4\text{-MeOppy})_2(\text{bpy})](\text{PF}_6)$ **2a** recorded at 298 K at 50

mV/s in MeCN with 0.1 M ($n\text{Bu}_4\text{N}$) PF_6

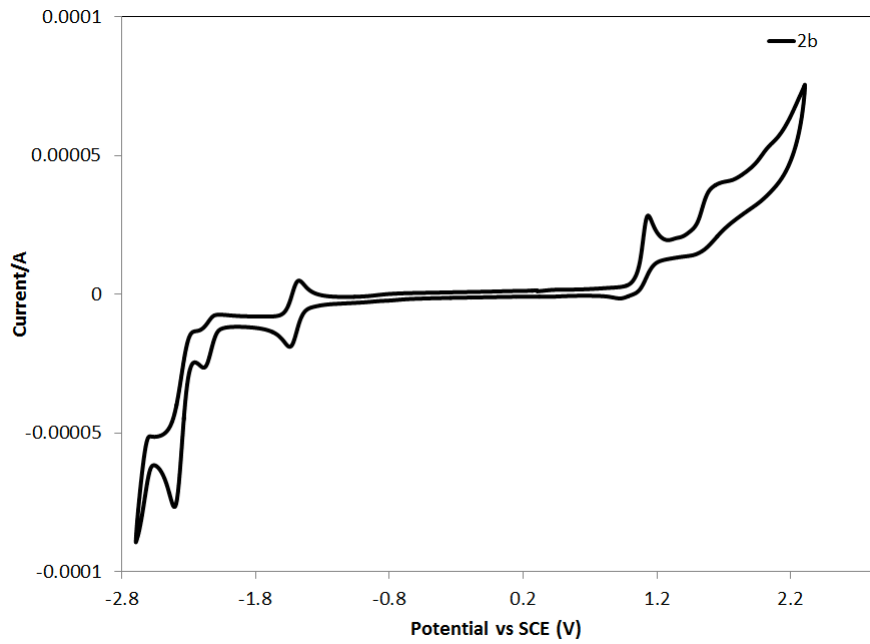


Figure S34. Cyclic voltammogram of $[\text{Ir}(4\text{-MeOppy})_2(\text{dtbbpy})](\text{PF}_6)$ **2b** recorded at 298 K at 50

mV/s in MeCN with 0.1 M ($n\text{Bu}_4\text{N}$) PF_6

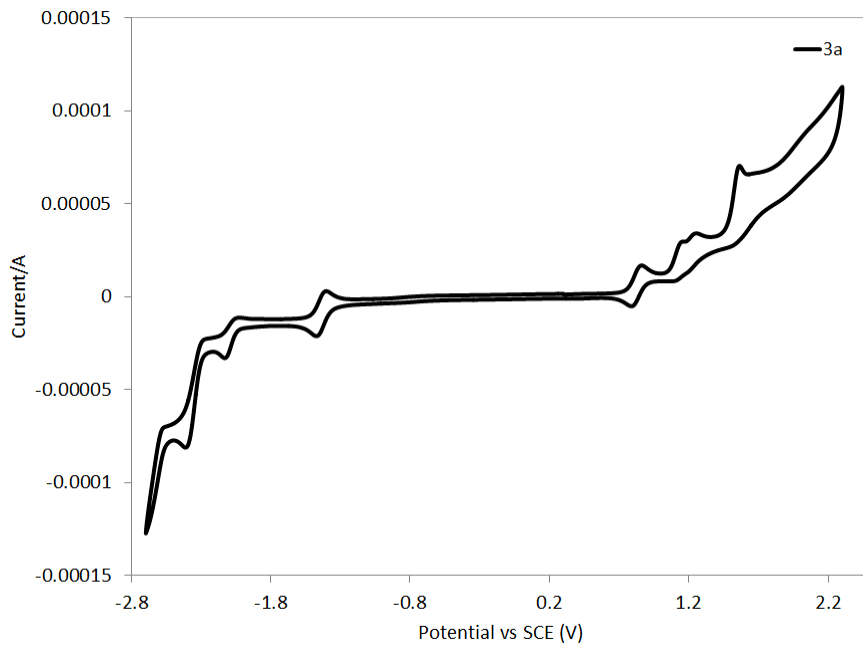


Figure S35. Cyclic voltammogram of $[\text{Ir}(3,4\text{-dMeOppy})_2(\text{bpy})](\text{PF}_6)$ **3a** recorded at 298 K at 50 mV/s in MeCN with 0.1 M ($n\text{Bu}_4\text{N}$) PF_6

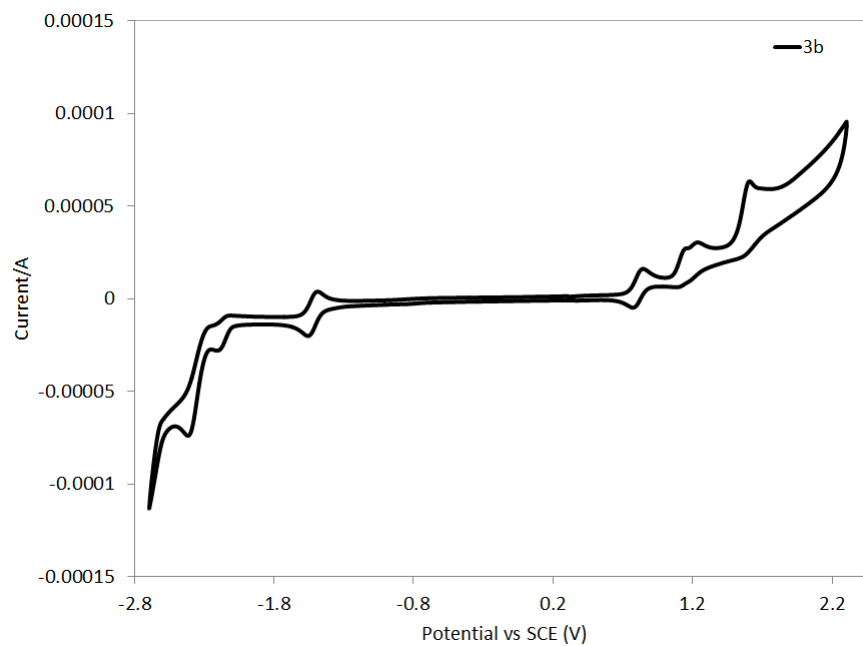


Figure S36. Cyclic voltammogram of $[\text{Ir}(3,4\text{-dMeOppy})_2(\text{dtbbipy})](\text{PF}_6)$ **3b** recorded at 298 K at 50 mV/s in MeCN with 0.1 M ($n\text{Bu}_4\text{N}$) PF_6

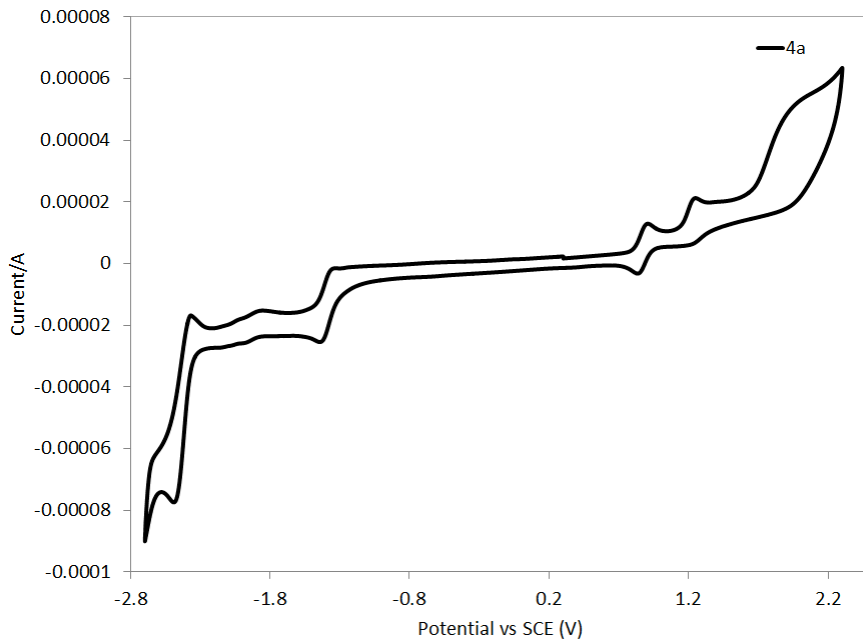


Figure S37. Cyclic voltammogram of $[\text{Ir}(3,4,5\text{-tMeOppy})_2(\text{bpy})](\text{PF}_6)$ **4a** recorded at 298 K at 50 mV/s in MeCN with 0.1 M ($n\text{Bu}_4\text{N}$) PF_6

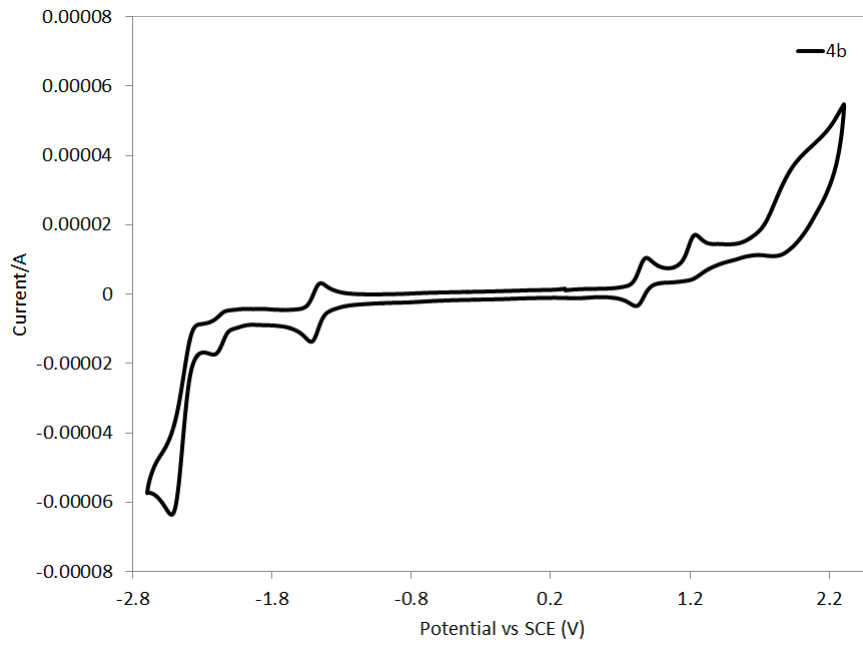


Figure S38. Cyclic voltammogram of $[\text{Ir}(3,4,5\text{-tMeOppy})_2(\text{dtbbipy})](\text{PF}_6)$ **4b** recorded at 298 K at 50 mV/s in MeCN with 0.1 M ($n\text{Bu}_4\text{N}$) PF_6

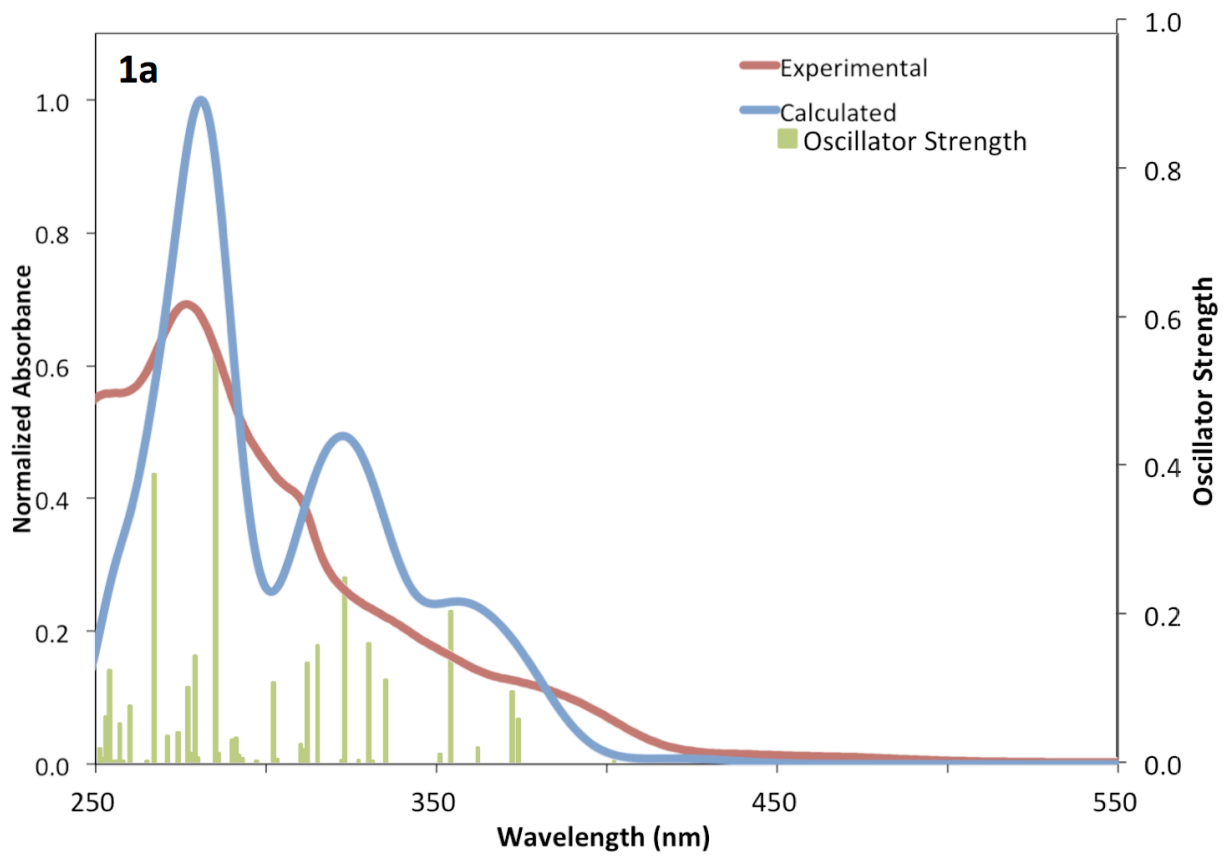


Figure S39. Experimental (red) and calculated UV-Vis spectrum (blue – fwhm = 1000 cm^{-1}) obtained from TDDFT calculations with the corresponding vertical excitations (green) for **1a**.

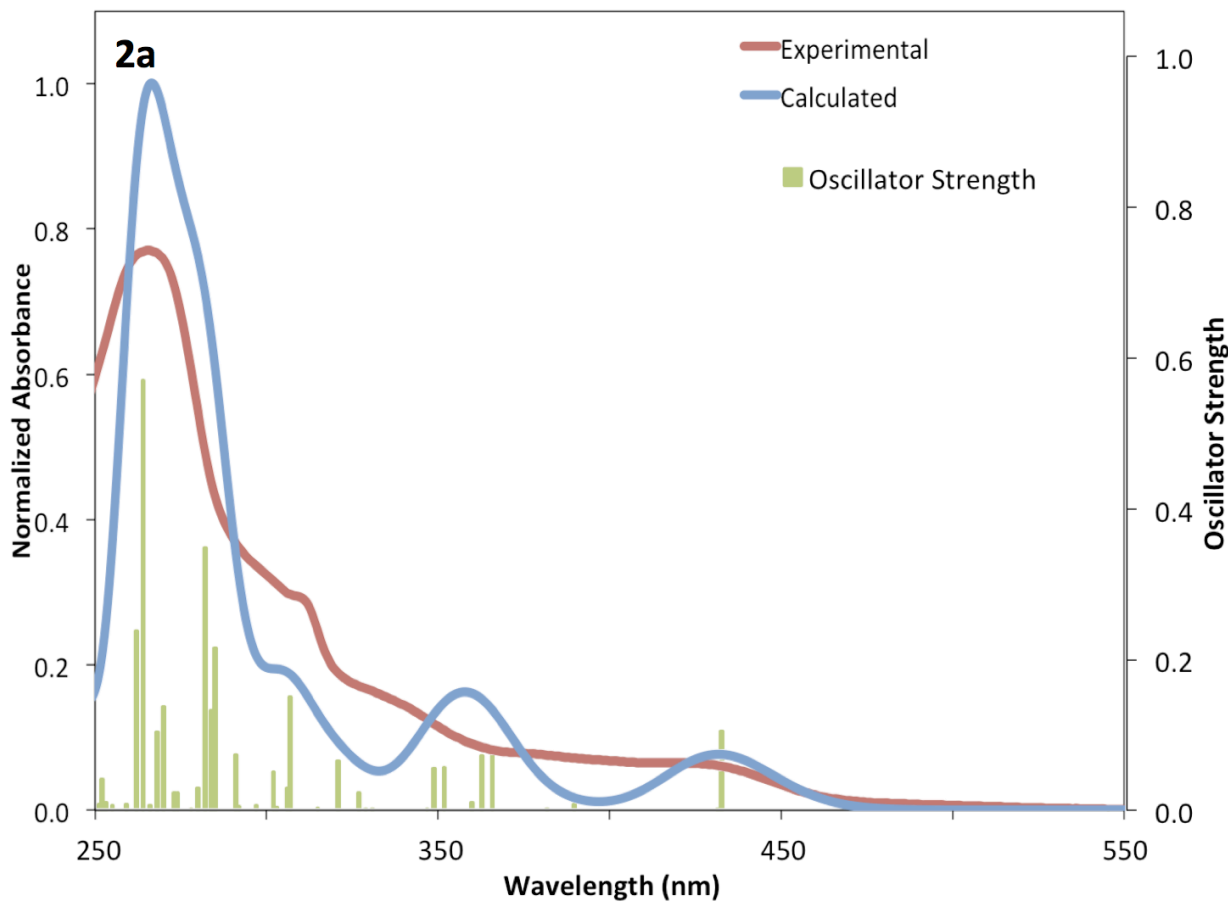


Figure S40. Experimental (red) and calculated UV-Vis spectrum (blue – fwhm = 1000 cm^{-1}) obtained from TDDFT calculations with the corresponding vertical excitations (green) for **2a**.

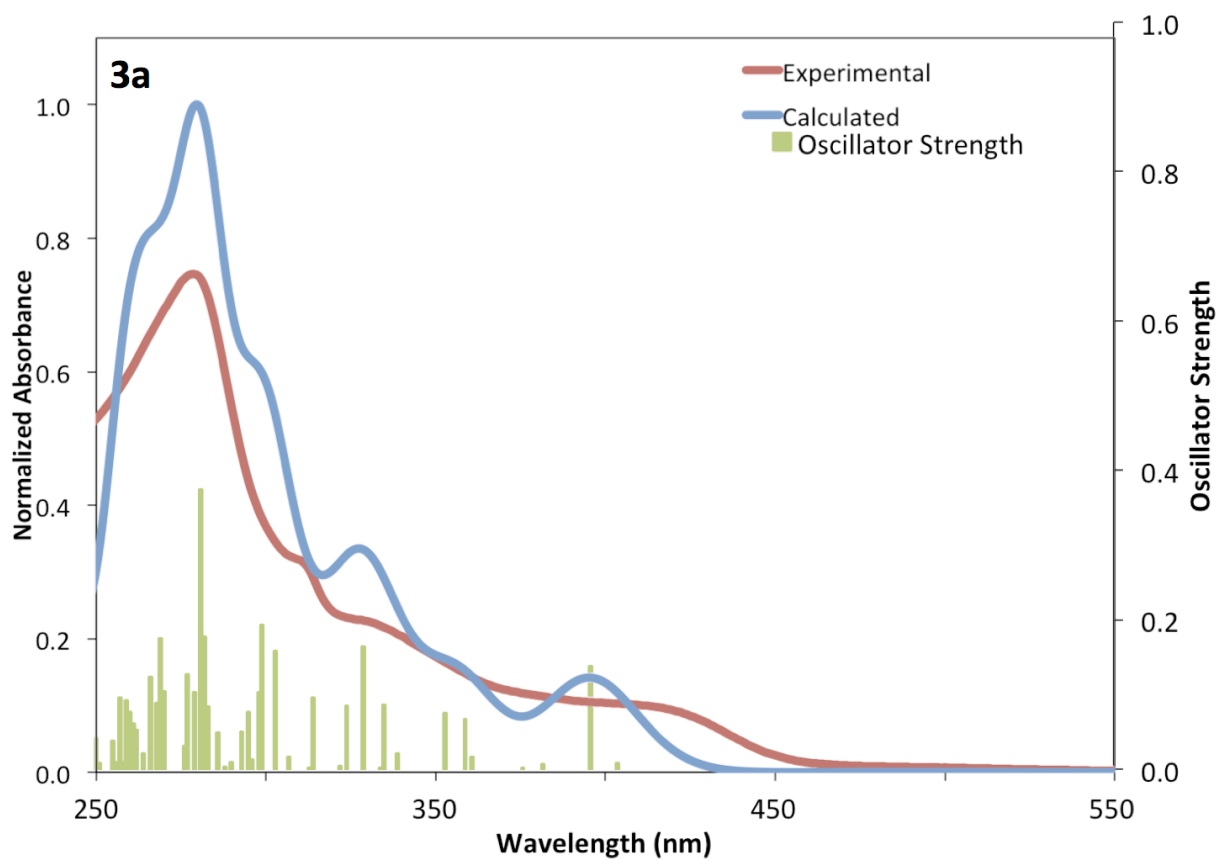


Figure S41. Experimental (red) and calculated UV-Vis spectrum (blue – fwhm = 1000 cm^{-1}) obtained from TDDFT calculations with the corresponding vertical excitations (green) for **3a**.

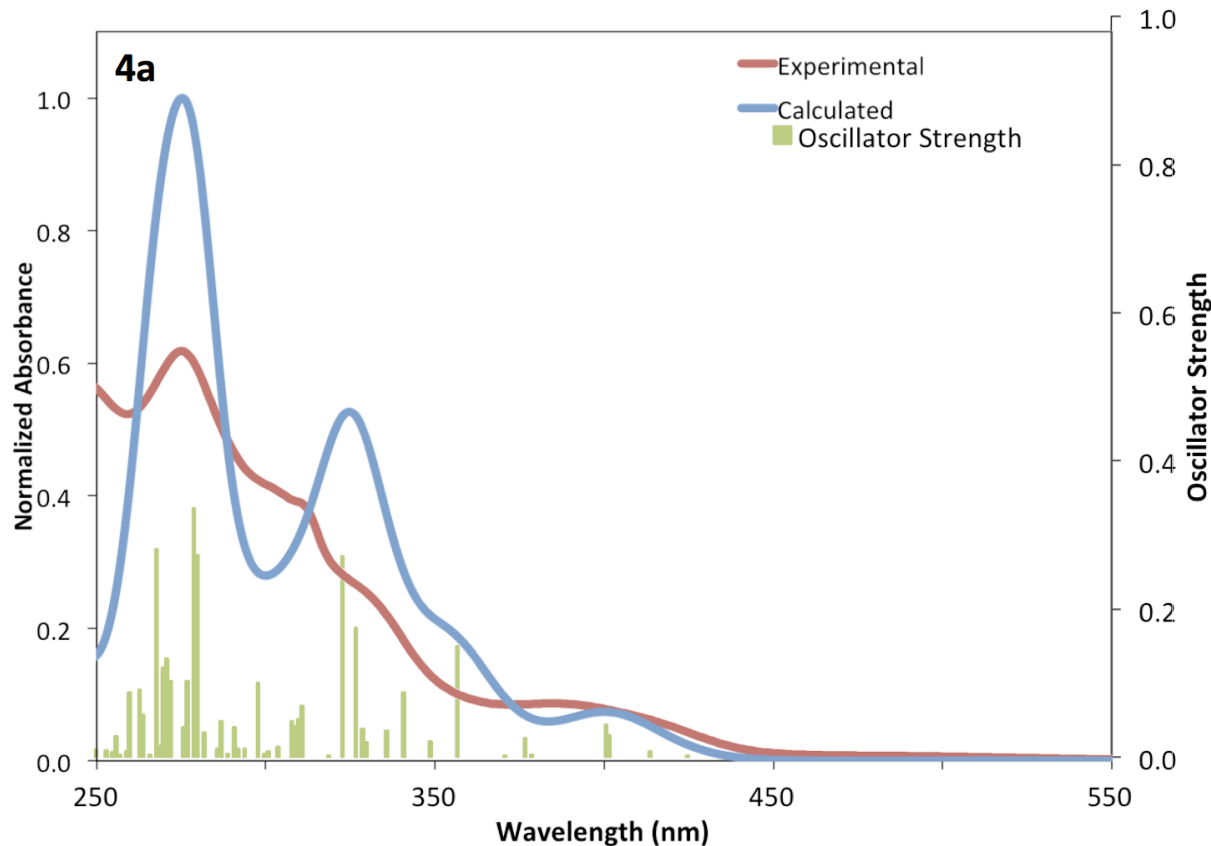


Figure S42. Experimental (red) and calculated UV-Vis spectrum (blue – fwhm = 1000 cm⁻¹) obtained from TDDFT calculations with the corresponding vertical excitations (green) for **4a**.

Table S3. Triplet state energies obtained by TDDFT.

	State	λ /nm	E/eV	Assignment [f]	Nature
1a	T_1	550.7	2.25	H→L (98%) [0]	$^3\text{MLCT}/^3\text{LLCT}$
1b	T_1	513.4	2.41	H→L (98%) [0]	$^3\text{MLCT}/^3\text{LLCT}$
2a	T_1	483.8	2.56	H→L (91%) [0]	$^3\text{MLCT}/^3\text{LLCT}$
2b	T_1	454.7	2.73	H→L (91%) [0]	$^3\text{MLCT}/^3\text{LLCT}$
3a	T_1	499.6	2.48	H→L (97%) [0]	$^3\text{MLCT}/^3\text{LLCT}$

3b	T_1	469.0	2.64	H→L (97%)	$^3\text{MLCT}/^3\text{LLCT}$
4a	T_1	524.1	2.37	H→L (97%)	$^3\text{MLCT}/^3\text{LLCT}$
4b	T_1	491.0	2.53	H→L (97%)	$^3\text{MLCT}/^3\text{LLCT}$

The most important parameters for the **1b** - **4b** based LEECs are shown in Table S4. The molecule **1a** did not work correctly and no electroluminescence data can be provided.

Table S4. Performance of LEEC devices driven at a constant voltage of 4V.

	t _{max} (s) ^a	Luminance _{max} (cd m ⁻²)	t _{1/2} (s) ^b	Efficacy (cd A ⁻¹)	Power Efficiency (lm W ⁻¹)	EQE (%) ^c	CIE _{x,y}
1a	-	-	-	-	-	-	-
1b	17	7.4	60	$6.7 \cdot 10^{-4}$	0.037	0.0005	0.56, 0.44
2a	3	53.1	30	$38 \cdot 10^{-4}$	0.0144	0.002	0.49, 0.50
2b	7	4.6	42.7	$6.3 \cdot 10^{-4}$	0.0004	0.0003	0.46, 0.52
3a	30	3.3	100	$4.5 \cdot 10^{-4}$	0.0002	0.0004	0.56, 0.44
3b	14	7.34	233	$8.6 \cdot 10^{-4}$	0.0005	0.001	0.57, 0.43
4a	8h	21	16h	0.029	0.007	0.034	0.63, 0.37
4b	1.1h	18	2h	0.050	0.013	0.050	0.61, 0.38

^a Defined as the time to reach the peak luminance. ^b Time to reach half of the maximum luminance. ^c External Quantum Efficiency.

References

- 1 Pavlishchuk, V. V. & Addison, A. W. Conversion constants for redox potentials measured versus different reference electrodes in acetonitrile solutions at 25°C. *Inorg. Chim. Acta* **298**, 97-102, doi:10.1016/s0020-1693(99)00407-7 (2000).